COMPARATIVE EVALUATION ON STATOR INSULATION METHODOLOGIES OF OLD LAXAPANA PRIOR AND AFTER REHABILITATION

Nadeesha Chathuri Manamperi

(109235V)

Degree of Master of Science

Department of Electrical Engineering

University of Moratuwa
Sri Lanka

June 2015

COMPARATIVE EVALUATION ON STATOR INSULATION METHODOLOGIES OF OLD LAXAPANA PRIOR AND AFTER REHABILITATION

Nadeesha Chathuri Manamperi

(109235V)

Dissertation submitted in partial fulfillment of the requirements for the degree Master of Science

Department of Electrical Engineering

University of Moratuwa
Sri Lanka

June 2015

Declaration of candidate and the supervisor

“I declare that this is my own work and this dissertation does not incorporate without acknowledgement any material previously submitted for a Degree or Diploma in any other University or institute of higher learning and to the best of my knowledge and belief it does not contain any material previously published or written by another person except where the acknowledgement is made in the text.

Also, I hereby grant to University of Moratuwa the non-exclusive right to reproduce and distribute my dissertation, in whole or in part in print, electronic or other medium. I retain the right to use this content in whole or part in future works (such as articles or books).

Signature: Date:

The above candidate has carried out research for the Masters Dissertation under my supervision.

Signature of the supervisor: Date:

Signature of the supervisor: Date:

Abstract

Key words: Stator**,** Ground wall insulation, Global Vaccum Pressure Impregnation, Vacuum Pressure Impregnation

All the hydro and thermal generators belonging to Ceylon Electricity Board, Sri Lanka are manufactured according to the Vacuum Pressure Impregnation (VPI) process except for the three new generators installed in Old Laxapana Power Station during the recent rehabilitation project (2012/2013). These three units replaced the previously existed VPI generators. The manufacturing process utilized for these generators is known as Global Vacuum Pressure Impregnation (GVPI). Even though GVPI process is more economical and offers many advantages, several cases of premature failures of GVPI generators have been reported worldwide. This influenced carrying out this study to assess the insulation condition of GVPI insulation comparatively with the VPI insulation. One new GVPI stator and two VPI stators were selected as test specimens. Removed stator of Old Laxapana and newly installed stator of Wimalasurendra Power Stations were selected to represent VPI insulation. During this research, the condition of the GVPI Stator was evaluated using the DC ramped high voltage test and Frequency Domain Spectroscopy (FDS) test. A mathematical model that has been established by both local and international research was utilized for separating the current components of the total measured current of the DC ramped high voltage test. By the current component separation it could be observed that minimum absorption current was required for the new GVPI insulation, which is an indication of superior quality of the insulation. The FDS test revealed important information of the dielectrics in the low frequency region. The results proved that minimum dielectric loss and minimum moisture absorption of all the three samples was for the GVPI insulation. The new VPI insulation had losses and moisture absorption lesser than the old VPI stator but nevertheless it could not match the low values of the GVPI insulation. Hence it could be clearly concluded that the GVPI insulation has better performance over VPI insulation.

Acknowledgement

My sincere thanks go to my supervisor (who is also my superior officer), Eng. G.A.Jayantha, Deputy General Manager (Generation Projects) of Ceylon Electricity Board (CEB), for his continuous guidance from the beginning to the end of this research. My thanks extend to Eng. G.A. Jayantha for providing me more than enough reading materials, which made me well equipped with the knowledge, for providing opportunities to work with colleagues researching on the same topic and most importantly for providing all the authoritative permissions to test the generators belonging to Ceylon Electricity Board. In simple, it would not be possible to end up this research a success, without his support.

My thanks are due to Prof. J.P.Karunadasa , my supervisor from the university, for the continuous encouragement and the guidance that made me move on with the project disregard of many bottlenecks.

I am grateful to the Engineers of Asset Management, Thermal, Electrical and Hydro Electrical branches of CEB for carrying out the specific tests required for this research amidst their busy schedules and providing novel ideas to enrich the scope of my research.

I thank to Engineers of Laxapana complex, Ceylon Electricity Board who helped to make my work a success, in many ways.

I thank my parents who always stood behind my every success, for their love and encouragement which always made me so strong.

Lastly I should thank many individuals, friends and colleagues, who have not been mentioned here personally, but supported me in making this educational process a success. May be I could not have made it without your support.

Table of Contents

List of Figures

List of Tables

Abbreviations

AC	- Alternating Current
AESIEAP	-Association of the Electricity Supply Industry of the East Asia and West Pasific
CEB	-Ceylon Electricity Board
DC	-Direct Current
DIRANA	-Dielectric Response Analyser
ELCID	-Electromagnetic Core Imperfection Detection
FDS	-Frequency Domain Spectroscopy
GVPI	-Global Vacuum Pressure Impregnation
IEC	-International Electrotechnical Commission
IEEE	-Institute of Electronic and Electrical Engineers
kV	-Kilo Volts
MW	-Mega Watts
OLPS	-Old Laxapana Power Station
PD	-Partial Discharge
RMSE	-Root Mean Squared Error
SSE	-Sum of Squared Errors
UK	-United Kingdom
VPI	-Vacuum Pressure Impregnation
WPS	-Wimalasurendra Power Station

List of Appendices

1. INTRODUCTION

1. 1 Background

Ceylon Electricity Board (CEB), the authority empowered to generate, transmit and distribute electricity in Sri Lanka, holds the ownership of 17 Hydro Power Stations which constitute 35 Hydro Generators. Oldest Hydro Power Station of them is known as Old Laxapana (Stage I), commissioned in 1950. After 62 years from commissioning, three units of Old Laxapana power station (OLPS) were rehabilitated with the aim of improving the efficiency and the reliability of the aged power station. However the stator windings of the Old Laxapana generators had been replaced once before in 1979 due to a severe failure.

CEB has been engaged in rehabilitating its' aged hydro plants, starting from Ukuwela then continuing to Wimalasurendra, Old Laxapana and New Laxapana power stations. Table 1.1 summarizes the periods that the plants had been in operation and periods of rehabilitation.

Table 1.1: Service and rehabilitation periods for hydro power stations of CEB

Power Station	**Service period**	**Rehabilitation period**
Ukuwela	1976-2010	2010 -2011
Wimalasurendra	1964-2011	2011-2012
Old Laxapana	1950-2012	2012-2013
New Laxapana	1974-2011	2011-2014

In all these rehabilitation projects, the original generators were replaced with new Generators of Class F Insulation.

When rehabilitating the Old Laxapana generators, the existed stator windings were replaced with new ones manufactured according to the latest insulation methodology. This insulation manufacturing methodology is known as Global Vacuum Pressure Impregnation (GVPI). Hence 11kV, 9.5 MW, form wound, Old Laxapana new generator stator windings have become first of the GVPI stators installed in Sri Lanka. Epoxy mica insulation system is manufactured to meet class F requirements. The Contractor for this project was Voith Hydro Kraftswork AG, Austria.

In a Global Vacuum Pressure Impregnation Process, half saturated coils are inserted to the slots and all connections are made. Then the vacuum impregnation process is done to the completed stator including winding and core. Hence the process is called Global Vacuum Pressure Impregnation system. Even though GVPI stator insulation has its known advantages, some cases have been reported worldwide of their premature failures. Site repairs for this kind of insulation failure are very difficult.

This study was done to evaluate the GVPI insulation system comparatively with Vacuum Pressure Impregnation (VPI) insulation system, which had been used in Old Laxapana generators that existed prior to rehabilitation as well in all other thermal and hydro generators belonging to CEB.

1.2 Literature Survey

Stator winding insulation, which is considered as the most susceptible part of a generator, is directly related to the performances of the Generator. It has been revealed that 56% of the generator failures occur due to insulation failures [1, 2].

For evaluating an insulation system it is vital to identify types of stator construction and the components and their purpose of use.

1.2.1 Types of stator winding construction

Two main stator winding construction methods have been practiced and developed by the manufacturers. They are known as random-wound and form-wound stator constructions.

1.2.2 Random wound stators

In random wound stators, insulated copper conductors are wound continuously through the slots in the stator core. The term ‘random’ wound is used for this construction because in these stators, each turn could be placed against any other turn in the coil independently from the voltage of each turn. It implies that it is possible that phase end turn is placed adjacent to the neutral end turn. Therefore this type of construction is used for operating voltages less than 1000 V [3].

1.2.3 Form wound stators

Form wound stators come in two different types. They are,

- Form wound stators using multi turn coils
- Form wound stators using roebel bars

1.2.3.1 Form wound stators using multi turn coil

Form wound stators are made of insulated coils which are pre-formed prior to inserting to the slots as shown in figure 1.1. The pre-formed coil consists of turns of diamond shape. Several coils are connected in series to create the proper number of poles and turns between the phase and the neutral. They are carefully designed to ensure that each turn has smallest voltage difference with the adjacent turn. This design requires very thin insulation between turns. Hence the stators of higher voltages are not unnecessarily bulky with the insulation. This type of stator constructions are used for higher operating voltages [3]. Old Laxapana and Wimalasurendra newly installed stators are of this type of construction.

Figure 1.1 : Form wound coils of Wimalasurendra power station 'original in color'

1.2.3.2 Form wound stators using roebel bar

As the generator output increases, the coils have to be manufactured larger and stiffer to carry higher currents. When the coils are very large it becomes very difficult to insert both sides of the diamond in to the core slots simultaneously without making any mechanical damage to the coil as well to the core. Therefore large generators are made using half diamond coils as shown in figure 1.2 and these are referred to as roebel bars. With roebel bar construction only one half of a diamond is inserted to the slot at a time and this avoids the difficulties in inserting two sides of the coils simultaneously. When using roebel bars, electrical connections need to be done on both ends.

Figure 1.2 : Roebel bar windings of New Laxapana stator 'original in color'

To avoid circulating currents within the winding due to different voltages induced within the strands, the strands are transposed regularly as seen in figure 1.3 to compensate currents which could cause circulating currents in the strands.

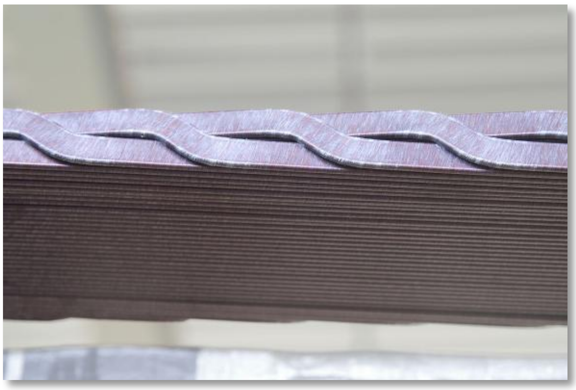

Figure 1.3 : Transposition of roebel bars ‘original in color’

Source: (http://en.partzsch.de/stator-windings)

1.2.4 Features of stator winding insulation system

The purpose of the insulation system is to separate the conductors from each other and the grounded core of a stator from the conductors. Design and material selection for stator insulation system has been evolved since the time of First World War.

A stator winding insulation system consists of following main features.

i. Strand insulation
ii. Turn insulation
iii. Ground wall insulation
iv. Slot corona protection layer
v. End corona protection layer

1.2.4.1 Strand insulation

Generator windings are stranded due to several mechanical and electrical reasons. Large single conductors are difficult to bend to obtain the diamond shape hence it is mechanically advantageous to form wound the coil in several strands as seen in figure 1.4. From electrical point of view, it is a known fact that as the conductor cross section increases, alternating currents tend to flow in the periphery of the conductor rather in the center of the conductor, which is called skin effect. Hence the effective cross section area of the conductor is less than the actual. Due to this scenario, the effective AC resistance is higher than the DC resistance. Therefore I^2R losses caused is larger in a large conductor [3].

Even though the main magnetic field is radial in the slots, an axial magnetic field is experienced by the end windings due to the abrupt ending of the rotor and the core. This magnetic field creates circulating current within the cross section of the conductor resulting I^2R losses [3].

In order to reduce the above two kinds of losses it is always preferred to use stranded conductors instead solid conductors with larger cross section. Figure 1.4 shows a cross section of OLPS stator winding in which the strands could be clearly seen.

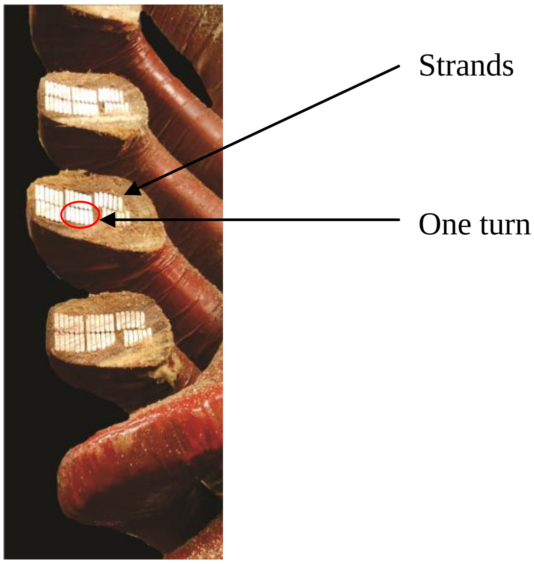

Figure 1.4 : Cross section of OLPS stator with six turns and six strands per turn 'original in color'

The strands used in a winding need to be insulated. Generally, the voltage between strands is small and therefore does not require thick insulation. Yet, as the strand insulation is the immediate layer after the current carrying conductor, where I^2R losses are mostly generated, this should have very good thermal conductivity [3].

During the manufacturing process it is required to bend and from the coils hence the strand insulation should have good mechanical properties as well. It had been the common practice to use single layer of ½ lap epoxy coated glass tape and one layer of mica tape of ½ lap as the strand insulation in epoxy mica insulation for the earlier version of generators. Latest trend is to use an insulation varnish coating of sufficient thickness which does not crack during bending.

Few strand insulation failures does not cause winding to fail, but it could lead to increased winding losses and increased local temperatures in a winding.

1.2.4.2 Turn insulation

Purpose of turn insulation is to avoid the inter turn shorts in a winding. If a short occurs between two turns, then that turn will behave as a secondary winding of an auto transformer. For example, if a winding has hundred turns between the phase terminal and the neutral terminal, and a winding short occurs in one turn, then that shorted turn will carry hundred times lager current than the normal current.

This is explained by transformer law,

$$N_s I_s = N_p I_p \tag{1.1}$$

Where N_s and I_s refer to the number of turns and the current in the secondary respectively. Similarly N_p and I_p refer to primary side turns and current [3].

In such case a large current will flow in the shorted turn rapidly overheating it. This will follow an earth fault as the copper and the turn insulation will get melted due to the excessive temperatures generated due to large current circulating. Therefore effective turn insulation is vital for a long stator life. In addition to the expected voltage difference between each turn, the turn insulation design should be able to withstand the surge voltages due to lightning stroke. Lightning strokes are earthed through surge arrestors but the residual voltage of the lightning stroke appears at transformer. This residual voltage is further attenuated when it travels through the power transformer. Therefore surge on the turn insulation of high voltage side of the generator is in the range of 1.5 times the line voltage if the surge arrestors are rated and working properly. This value is considered in designing the turn insulation of the line terminal coil. Practical experience shows that for 13.8 kV generator insulation is made of 4 layers of ½ lap mica tapes.

1.2.4.3 Groundwall insulation

Groundwall insulation is used for the purpose of insulating the copper conductors from the grounded core. For a long service life, the groundwall must be able to stand up of electrical, mechanical and thermal stresses that it is subjected to.

The full rated phase to phase voltage is applied across the groundwall only at the phase end of the winding and this requires substantial ground wall thickness. The same thickness is not required at the neutral end of a winding, as no voltage is applied across the ground wall there, during normal operation. Despite of that fact, normal practice of manufacturers has been to continue with same insulation thickness over the whole circumference. In an indirectly cooled form-wound machine, main path of heat transfer from copper conductors to the stator core is through the groundwall. To achieve a good heat transfer, the materials used for groundwall should have higher thermal conductivity. One important aspect during manufacture of the groundwall is to make sure air pockets are not formed in it, because existence of the air pockets creates a considerable obstruct to the heat transfer path [3].

The conductor vibration is a natural phenomenon in a generator, which occurs due to the magnetic forces. The groundwall should have a good mechanical strength to prevent insulation abrasion due to vibration. Therefore groundwall materials should be very incompressible, where it would support to prevent the vibration of the turns and strands against each other.

1.2.4.4 Slot corona protection layer

As the coils and bars are fabricated outside the core, they must be thinner than the slot width, in order to be inserted to the slot. Thus an air gap between the coil/bar and the slot is inevitable [3].

Slot corona protection layer is a semi conductive tape layer/coating used to provide better contact with the ground wall. If the electric stress in this air gap exceeds 3kV/mm, which is the breakdown voltage of air, partial discharges would begin to occur, which will gradually cause the groundwall to fail. Therefore manufacturers have been coating the coil/ bar area in the slot with semi conductive coating. This is usually a carbon-black-loaded paint or tape as shown in figure 1.5.

Figure 1.5 : Applying semi-conductive tapes to the roebel bars at New Laxapana 'original in color'

This coating cannot be highly conductive, because such coating will short the core laminations. The semi conductive coating will contact with the groundwall insulation in many places along the slot portion. As shown in figure 1.6, higher voltages across air pockets will not develop due to the low resistance (Rs) of the coating. C_a is the capacitance across the air gap.

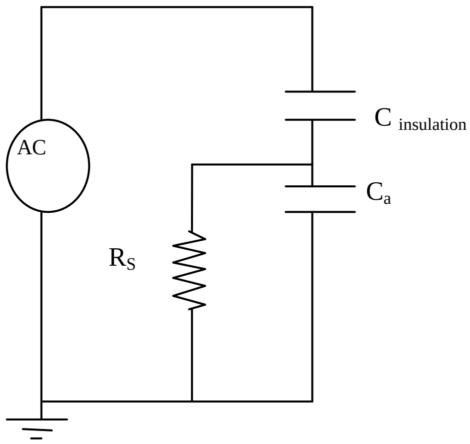

Figure 1.6 : Equivalent electrical circuit for bar/coil with semi conductive coating

1.2.4.5 End corona protection layer

The semi conductive coating is applied only few centimeters outwards from the end of the slot portion. This thin coating cannot be suddenly ended, as localized higher electric stresses are subject to build at such locations. If this field exceeds 3kV/mm, partial discharges would begin to occur. The stress grading tape/end corona protection layer is used for the purpose of relieving the electrical stresses at the end of the semi conductive layer [3].

The stress grading tapes are coated with Silicon Carbide (SiC), which has the special property of reducing its resistance as the electric stress increases. Thus when applied to a copper coil/ bar it provides a minimum resistance at the high stress regions at the end of the semi conductive coating and gradually increases its resistance along the end winding from the core. Silicon Carbide can be used as paint base, or incorporated to a tape.

1.2.5 Evolution of the insulation materials

1.2.5.1 Asphalt Mica

First generator insulation systems used in the world used Asphalt Mica, which was formed using natural materials. Asphalt contains a wide variety of molecular sizes of predominantly long, straight chain hydrocarbons with a high degree of saturation and with some sulfur, nitrogen and oxygen.

Insulation system from Asphaltic resins combined with mica splittings were first developed during the period of First World War. It was first introduced by the General Electric Company in 1915.To use as an insulation, the mica splittings were supported on cellulose papers and impregnated with Asphalt varnish [4].

Asphalt is a thermoplastic material. Thermoplastic materials are solids that soften and melt upon heating. When cooled it again solidifies. Use of Asphalt was restricted only for Class B (130 ^{0}C) applications due to the reason that formation of permanent and continuous carbonised cracks could occur in Asphalt at very high temperatures. This may lead to increase in dielectric losses and finally groundwall insulation failure. Even though Asphalt exhibits good resistance to transmit moisture, moisture ingress could happen if cracks and fissures exist. Groundwall failure at or near the ends of stator core are commonly observed failure modes for Asphalt insulated generators. Compound migration and tape separation caused by differential thermal expansion and thermal cycling is the main reason for such failures which are also called as ‘girth cracks’ [5].

The average withstand voltage of Asphalt mica is controlled to be less than the partial discharge voltage of the voids. Hence the average withstand voltage of Asphalt mica insulation is generally designed to be less than 2 kV/mm [4].

1.2.5.2 Polyester

Polyester is a synthetic resin which first became available in 1942, during the World War II [3]. It is the first thermoset material used in generator stator insulation. Thermoset is a polymer which is cured by heat or chemical reaction and becomes infusible or insoluble material. Polyester was introduced as a result of the increasing demand for insulation materials which can operate well in higher temperatures and voltage gradients. It can be used for both 130^{0}C and 155^{0}C temperature classes [5]. Research work are in progress to develop the polyester resins to be used for temperature class 180 ^{0}C. It is inexpensive but the main disadvantage of polyester resins is that in some parts of the carbon chain have oxygen atoms double-bonded to carbon atoms, forming permanent dipoles which increases the capability of absorbing moisture.

With Polyester resin, the groundwall insulation is designed to withstand a stress level of 5kV/mm.

1.2.5.3 Epoxy Resins

Epoxy resins were first commercially available in 1947[4].Epoxy resin insulation systems had advantages of improved thermal stability and less contraction during hardening compared to polyester resins. General Electric Company obtained the patent license for Epoxy-mica paper and resin rich insulation technology [4].

Epoxy is also a thermosetting insulation material. Epoxy resins are non-polar, mechanically strong, and highly resistant to chemical attack and moisture absorption. It is well adhesive to most materials, and they have no by-products of formation. Epoxy is more expensive than polyester resins and requires more careful control of the curing process in which the cross-linking is formed. Epoxies cure to a stronger polymer that has improved thermal stability. Shrinking on hardening is also less for epoxies when compared with polyesters [4].

Epxy resins are designed to withstand 5 kV/mm stress level and it is the currently preferred type for high voltage stator insulation.

1.2.5.4 Modern Systems

After the license of General Electric Company ran out, other companies developed their own systems.

1.2.6 Evolution of Insulation Methodologies

Ever since the introduction of Asphalt Mica in 1915, the insulation methodology used was known as Vacuum Pressure Impregnation system [4]. It was known as the corner stone of the Generator insulation systems used worldwide. Global vacuum Pressure Impregnation system was an advancement of this system and it was introduced in 1960s [4].

1.2.6.1 Vacuum pressure impregnation system

The tapes for vacuum pressure impregnation (VPI) are usually mica paper tapes made with binder resin to fully saturate the insulation and to bond the layers of the tape. The binder resin is normally of the same resin family as the final impregnating resin. In some cases, the tape binder resin is used without a curing agent. The porosity of the tape layers allows the impregnating resin to flow through the entire structure, assuring that the proper amounts of curing agent is dispersed throughout the groundwall insulation . Tapes impregnated with insulation materials are then applied to the vacuum pressure process and this process is fully automated in modern factories. The insulated coils are put in a heated coil tank. A vacuum is applied to this tank to evacuate the remaining of the solvent, moisture, air and undesirable volatile materials. While under the vacuum, the entire coil batch is flooded with melted hot resins and tank is pressurized with nitrogen gas. The pressure is maintained for several hours for high voltage generators to force liquid resin to the insulation tape layers such that no voids are left. After venting excess Nitrogen gas and the remaining solvent is pushed back to storage, the hot coils are taken out of the tank and allowed to cool at the room temperature .Then the fully saturated coils are moved to curing process. The coils are put in an oven and heated to a temperature at which final polymerization and cure is made where the resin becomes a thermoset. Insulated coils are then inserted to the core slots and connections are made [4].

1.2.6.2 Global Vacuum Pressure Impregnation System

Global Vacuum Pressure Impregnation (GVPI) System which is an advancement step of VPI system was developed in 1960s [4]. This System is discussed in detail in Chapter 2.

2.1 Introduction - GVPI System

Global Vacuum Pressure Impregnation system or Post-VPI system was developed for making coils and bars with insulating tapes that are not fully saturated with resin and are not cured prior to insertion in the stator slots. In GVPI method, the soft coils (also called green coils) are more easily fitted into the stator, and all of the connections can be made before final impregnation of the windings.

This system is well suited to small and medium capacity hydro generators with rather short coils. For large generators with long and large coils this method is not suited because the initial coil/slot contact condition seems rather difficult to maintain over a number of years due to thermal expansions and shrinkages of the coils, resulting from frequent start/stop and adjustable load operations. However, large hydrogen cooled turbo generators up to 340 MVA and air cooled turbo generators up to 260 MVA has been manufactured according to GVPI method [6].

Material Tests are important for GVPI coils, which are not complete until the full wound machine is subjected to vacuum pressure impregnation process. Resin curing is highly important factor in this system.

2.2 Procedure for Global Vacuum Pressure Impregnation of Old Laxapana

2.2.1 Pre-GVPI process

The coils of form wound stator of Old Laxapana are made of insulated conductor wires. The turn to turn insulation is made by corona resistant polymer/mica combinations. First, the form wound coils are wrapped with porous mica tape to a thickness determined by the rated voltage to provide a durable groundwall insulation of high dielectric strength. Then the conductive corona protection tape is applied on the stator slot portion of the coils to avoid corona discharges in the stator slot. A semi conductive layer is applied to the coil overhang beginning at the slot exit in order to achieve uniform stress grading of the voltage to ground.

After applying the insulation taping, the un-impregnated soft coils are inserted in the stator slots. This flexibility ensures that the stator can be wound without damaging the coils. Highly resin absorbent fiberglass cords are used for the coil overhang support. Slot wedges are inserted to retain the coils firmly in the stator slots.

2.2.2 GVPI process

The stator core that has been wound with the un-impregnated coils is placed in a large tank and vacuum dried with heat for about 8 hours in order to remove moisture. Vacuum chamber is heated by flowing a heated liquid around the periphery of the vacuum chamber. Meanwhile in a separate chamber, the resin is heated to about 50^0C for approximately 3 hours. After applying the vacuum cycle, the wound stator is entirely flooded with melted resin. The vacuum chamber is pressurized to 6 bar with a nonreactive gas (Nitrogen) and kept for about 3 hours to drive the resin throughout the ground insulation and the coil-to-coil and phase-phase connection insulation. After the impregnation period, the unabsorbed impregnating resin is drained back to storage; the wet stator is placed in an oven and heated to 145 ^{o}C for 24 hours to cure the resin.

2.3 Advantages of GVPI System

The GVPI insulation system offers several advantages over VPI insulation system. The number of handling operations are less in GVPI system, compared to the VPI system. This makes it less labor and time intensive and results in lower manufacturing cost. Since the coils are glued to the stator core with resin, the reliability against loose windings is very high. This reduces maintenance associated with vibration problems. As the resin integrates the stator winding and core, no air gaps exist between winding and insulation. Hence thermal transmitting is improved and partial discharges are minimum in this kind of stators.

2.4 Disadvantages of GVPI System

The biggest disadvantage of GVPI insulation is that the site repairs are not technically and economically feasible unlike in VPI Insulation. In a VPI stator, a faulty winding section can be removed easily with minimum disturbance to the integrity of the core. Then the particular section can be repaired and re-installed. In a GVPI System, carrying out a site repair is extremely difficult as the coils are bonded tight to the core and nearly impossible to remove in a failure. Even if the coils are replaced with extensive effort, the GVPI impregnation cannot be made at site. When the repair is done at site using VPI coils, the stator insulation will be a combination of GVPI and VPI. In some cases site repairs of GVPI stators had been carried out. It requires special tools, special procedures and special skills. Re-wind is a slow process and even though performed the core is vulnerable to damage. Therefore a great debate exists among manufacturers whether a site repair is a genuine solution or not.

Several cases of premature failures of GVPI systems have been recorded worldwide [7]. In most of the cases, the failures were due to partial discharges and slot vibrations which are contradictory to the guarantee given by the manufacturers for less possibility of occurrence of partial discharges and vibrations in GVPI insulations. This could happen if the coils are designed too small for the slots. In such case when the coil is subjected to the load cycling stresses between the coils and core, loose coils and slot discharges can happen in such design [8].

It is difficult to detect the manufacturing defects of a GVPI stator, since only the entire stator, but not the individual coils can be tested after impregnation [8].Core defects cannot be identified by some important diagnostic tests such as Electromagnetic Core Imperfection Detection (ELCID) test. Test is not possible because the key bar and the core is insulated by the resin in a GVPI stator, hence no return path for back current.

2.5 Premature Failures and Site Repairs

Several cases of premature failures of GVPI stators were reported worldwide.

Case 1:

As reported by G. C. Stone in [7] two GVPI generator stators rated in the 200 MVA range have been rewound in-situ in 2008.

Case 2:

Three air cooled generators of 200 MVA, GVPI insulation, belonging to Public Power Corporation S.A. of Greece, which is the biggest power corporation in Greece had presented problems such as loosening inside the slot, partial discharges and damage of the corona protection. Three top bars had been replaced and the company had been seeking for a complete rewind [9].

Case 3:

As Clyde V. Maughan of Maughan Generator Consultants Company reports in [10], a site rewind of a Siemens GVPI unit was done in South America around 2007.

Case 4:

Padma Kumar of National Thermal Power Corporation of India has reported in [11], that 250 MW, GVPI generator belonging to their company had failed after six months of operation. In restart, during the voltage build up, the generator had tripped on differential and when inspected found that stator overhang charred.

Case 5:

Failure of a 5 MW GVPI type generator in Tenau Diesel Power Plant, Kupang, Indonesia had occurred due to partial discharges and over voltages. Site repair as shown in figure 2.1 had been carried out for five months and reported as a success after 35,000 hours running [12].

Figure 2.1 : Removing the damaged windings of GVPI stator at Tenau diesel plant

Source: (I. Rendroyoko et.al, AESIEAP Conference on Electric Supply Industry, 2010)

Case 6:

Failure of 200 MVA, 16 kV, 3000 rpm GVPI insulated turbo generator belonged to National Power, UK had been damaged due to bar looseness and slot discharges. The Generator was installed in 1993 and has failed in 1999 after about 35,000 hours of operation. Partial discharge (PD) data base has recorded PD level of 2187 mV in 1998 on B phase, though the failure was not due to PD activity [13].

Case 7:

Failure of a large air cooled GVPI stator of capacity 100.7 MVA and of generating voltage 13.8 kV, belonging to a geothermal power plant of Indonesia is reported. The generator had failed after 13 years of operation. After a bus duct phase to phase fault, cracks in surge supports were observed. Evidence of excess vibration on end windings and loose core were witnessed. After six years from the fault the GVPI stator core had failed catastrophically burning significant amount of core laminations. Windings had been removed by mechanical procedure. By screwing the top of each bar, lag bolts had been fixed. Lag bolts had been pulled using hydraulic jacks and bars had been taken out of the slot as shown in figure 2.2 [14].

Figure 2.2 : Removal of the winding bars using hydraulic jacks

Source: (B.Moore et.al, Conference on On-line Monitoring of Electrical Assets, 2014)

Since substantial amount of core had been damaged, 100% new stator laminations had been used to restack the core. Winding insulation was changed to vacuum pressure impregnation. Several design changes were done. In order to achieve good heat transfer similar to GVPI insulation, the bar design was carried out to reduce the losses. Roebel transposition of 360^{0} had been changed to 540^{0} and strand insulation was also changed to finally accomplish 4% reduction in losses [14]

2.6 Resin Injection

As a preventive maintenance action for the vibration sparking that can occur in GVPI stators, some consultants recommend resin injection every 17,000 to 25,000 hours [15]. This could reduce stator bar looseness happening at early stage of operation. Also it may reduce partial discharges and earth fault occurrences for some time. Effect of vibration sparking is shown in figure 2.3.

Figure 2.3 : Effects due to vibration sparking

Source: (http://www.generatortechnicalforum.org/portal/forum/viewthread.php?thread_id=48&fgroup=1)

2.7 General Procedure for GVPI Stator Rewinding

2.7.1 Repairing the core

The compression bolts and finger plates should be removed from the stator frame. After removing slot wedges, whole stator should be cleaned with dry air. Windings shall be removed from the core.

Separation of the damaged core laminations could be done by a thin knife. Once separated the individual lamination sheets shall be insulation varnish sprayed and dried. Before reinstalling the laminations, the damaged finger plates shall be repaired. Then lamination plates shall be installed and epoxy/resin shall be applied. Compression bolt shall be reassembled to the required torque and core looseness shall be tested and verified.

Insulation tests shall be carried out to test the core repair. Paint coating shall be applied prior to inserting the windings.

2.7.2 Repairing the windings

Damaged windings can be removed by high pressure water jets or hydraulic jacks. The excessive movement of coils can create cracks in certain parts of the winding. All the cracked windings have to be repaired and proper testing (Hipot etc.) shall be carried out for each coil. The voids in the slots shall also be filled with insulation at site. After rewinding, the stator shall be heated in order to remove moisture and tested to verify the condition. Since standards do not specify the test voltages for half saturated coils, appropriate criteria shall be utilized for acceptance of the test outcomes.

3. DIAGNOSTIC TESTS FOR INSULATION

For this study, two tests were used for assessing the condition of the insulation, namely DC ramped voltage test and frequency domain spectroscopy (FDS) test. DC ramped voltage test analysis is done in the time domain whereas FDS test analysis is done in the frequency domain. The two tests reveal independent details on the condition of the insulation.

3.1 DC Ramped Voltage Test

DC ramped voltage test is known as a very safe diagnostic test used to assess the insulation condition of the dielectric materials. It was first introduced by Bruce McHenry in 1964[5]. The test is simple and less time consuming. Many utilities worldwide have used high voltage DC ramp test for generator insulation assessment for over 40 years. In this test, voltage is ramped up (normally at a rate of 1kV/min) and the leakage current is plotted against voltage in real time. If a sudden increase of current is observed in the plot, the test can be interrupted immediately to prevent any possible failure. The instrument has emergency trip function to trip in case of a sudden flashover. DCR-50 Test set used for the assessment is shown in figure 3.1.

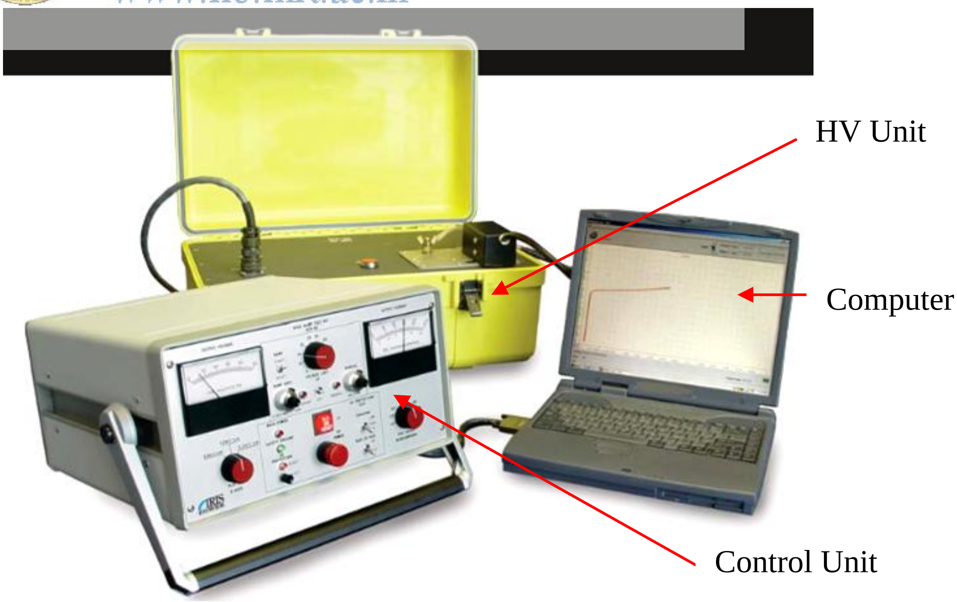

Figure 3.1 : DCR-50 Test Set

Source: (DCR-50 Flyer, IRIS Power)

The maximum voltage the high voltage source should be programmed to not to occur a current avalanche is determined as follows. As per IEC 60034-1, it is 2E+1kV [16]. Where, E is the rated AC line to line voltage. Hence applying the AC to DC conversion factor of 1.7, the maximum ramped DC voltage applied is sealed by (2E+1kV) x 1.7. According to IEEE 95-2002 standard, the AC test voltage for maintenance proofing shall be taken as 65% to75% of 2E+1kV [17].Hence applying the conversion factor, the DC voltage test value for maintenance tests is 1.7 times of the alternating voltage (rms) maintenance test value (50Hz/60 Hz). Therefore DC test voltage for an 11 kV stator shall be 25.415 kV to 29.325 kV.

Since there is a significant risk associated in subjecting the machine to such high stress, the maximum voltage level is normally not reached during the test. It is practically observed that adequate information can be gathered at fraction of above said high voltage limit. It is normal practice in Asset Management branch of Ceylon Electricity Board to limit the test voltage to 15 kV for 11 kV or 12.5 kV rated stator. The experience has proven that this voltage is sufficient to gather required information on the stator insulation. For aged windings even lesser voltage is applied.

There are several advantages in using DC voltage to test than AC voltage. Even though the stators are manufactured according to VPI/GVPI technologies, there are voids remaining inside the insulation. During AC cycles, arcing inside these voids can occur, which is known as partial discharge. When one void begins conducting, adjacent void starts arcing. Likewise possibility of avalanche breakdown can cause the stator winding to fail during an AC test. In a DC test reversing of the voltage cycles does not exist, which leaves no chance for such failure.

Since voltage is continuously increased during the test, the capacitive charging and the polarization effects are more similar to a low frequency AC test. A typical 20-minute ramped voltage test is roughly equivalent to a frequency of 0.2×10^{-3} Hz [5]. The sampling rate of the data acquisition unit is very high. For one test which takes about 15 minutes, total number of data points recorded is around 93,000.

3.1.1 Dielectric Phenomena

The current through the insulation is a resultant of three actions taking place inside the dielectric when high voltage is applied. The resultant current from DC ramped voltage test is the summation of capacitance charging (I_C), dielectric absorption (I_A) and leakage current (I_L) [5], [18]. The typical response curve of a DC ramp test is shown in figure 3.2.

The total current (I_t) measured in a DC Ramp Test shows a rapid increase initially due to capacitance charging current (I_C). Afterwards, absorption (I_A) and leakage (I_L) currents contribute to linear rise of the total current. The condition of the insulation can be analyzed if the three current components can be separated.

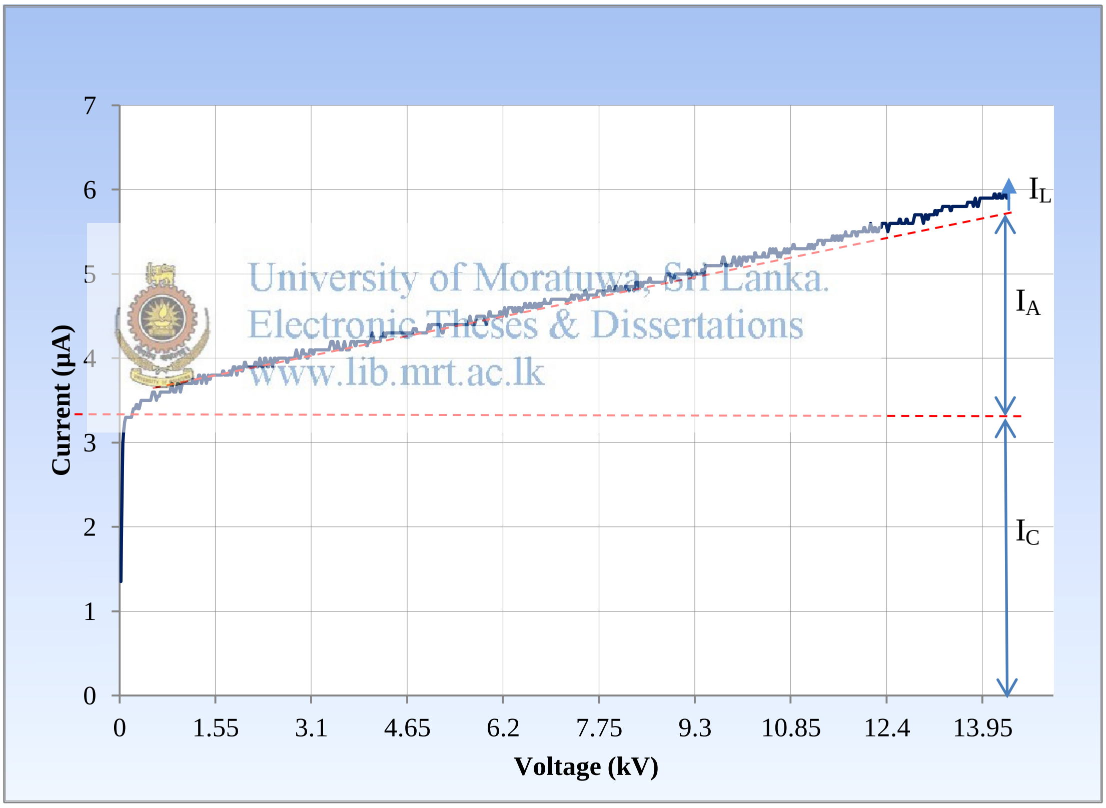

Figure 3.2 : Response curve of a DC ramp test

3.1.1.1 Capacitance charging current (Ic)

If the high voltage conductor coils of the stator winding and earthed core is placed in free space, it is charged up to its inherent capacitance which is owed to its geometry. This inherent capacitance due to geometry is called as geometrical capacitance. The geometrical charging current is the large current drawn at the moment of applying the DC Voltage to the insulation. It is given by the equation 3.1, where C_0 is the geometrical capacitance. The capacitive charging current can be considered constant since the dV/dt term is constant throughout the test.

$$I_c = C_0 \frac{dV}{dt} \qquad (3.1)$$

The geometrical charging current lags the applied voltage due to the surge limiting resistor of the equipment. This delay is visible by the slightly rounded shape at the beginning of the curve in figure 3.2.

Geometrical capacitance of a stator winding is proportional to the area of the plate (A) and inversely proportional to the distance between the two plates (d).

$$C_0 \propto \frac{A}{d} \qquad (3.2)$$

Hence this value is affected by the size, shape and the spacing between the conductor and core. Therefore this current is not considered for assessing the quality of the insulation. As I_C is constant throughout the DC ramp test, any fluctuations of total current measured is due to absorption or leakage current components.

3.1.1.2 Absorption current (I_A)

Dielectric material of a capacitor tends to neutralize the surface charges, thereby reducing the contribution to the electric field. It is caused by the elementary charges in the dielectric material with positive and negative polarities. These charges cannot move freely but can be displaced under an electric field. When a field is applied, the negative charges are shifted towards the positive electrode and the positive charges are shifted towards the negative electrode. Likewise, the dielectric neutralizes the surface charges of the electrodes to some extent reducing their contribution to the electric field [5].

This current drawn by the insulation to align the dipoles within the applied electric field is known as the absorption current. Absorption current is a characteristic of the basic substance. Increase of absorption current could be due to aging of material, aging of adhesive which bond mica together, oxidation aging, thermal aging or due to byproducts of partial discharges. Absorption current is a good indicator of the condition of the dielectric. The steepness of the slope of the V-I curve varies according to the absorption and leakage current drawn by the insulation material.

3.1.1.3 Leakage current (I_L)

Leakage current is the current through the impurities of the insulation. It can be considered as a summation of two components. Transverse component is due to the impurities of the dielectric and longitudinal component is due to surface leakages in the areas where winding is outside the magnetic core. The winding area outside the magnetic core is more sensitive to the moisture and surface pollution. Insulation in good condition shows minimum leakage current [5].

3.1.2 Test set-up

Test setup is shown in figure 3.3. Test was carried out for one phase at a time. The high voltage was applied to the winding and the current through the insulation was measured from the grounded stator frame. The neutral link was removed and other two phases were grounded. Test was carried out using DCR-50 instrument. Voltage was increased from 0-15kV at a rate of 1 kV/min and current vs. voltage plot was observed online.

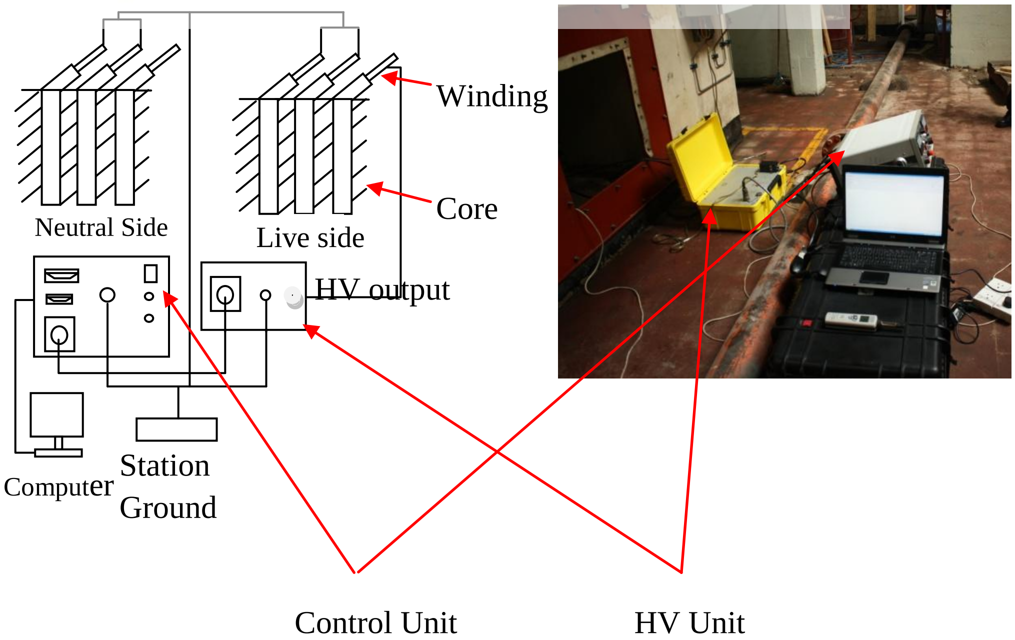

Figure 3.3 : Schematic and actual test set-up with DCR-50

3.1.3 Test specimens

Three generator windings were tested for comparison. The newly installed GVPI stator winding of Old Laxapana and old VPI stator winding of Old Laxapana were tested initially to compare the difference between two insulation methodologies, i.e. VPI and GVPI. It was understood that this comparison is not fair since one specimen being an aged winding. Hence a new specimen of VPI methodology was selected for testing. The VPI stator winding of Wimalasurendra Power Station is similar in winding construction (form wound multi turn coils) and similar in generating voltage (11 kV) to the Old Laxapana generators. It was newly installed in 2012.

Summary details of test specimens are given in table 3.1.

Table 3.1 : Summary of test specimens

Winding	Rated Voltage (kV)	Capacity (MW)	Insulation Class	Year of Installation	Insulation Methodology
Old Laxapana Unit 3 (before rehabilitation)	11	8.33	Class F	1979 (Epoxy mica glass)	VPI
Old Laxapana Unit 1 (after rehabilitation)	11	9.5	Class F	2013 (Epoxy mica)	GVPI
Wimalasurendra Unit 1 (after rehabilitation)	11	25	Class F	2012 (Epoxy mica)	VPI

3.1.4 Site tests

3.1.4.1 Testing of Old Laxapana VPI stator

Old Laxapana VPI stator was tested prior to its removal for the rehabilitation project. Voltage was increased at a rate of 1 kV/min up to a maximum voltage of 15 kV.

Current through the groundwall was measured. This winding had been in operation For 33 years since 1979. Figures 3.4, 3.5, 3.6 and 3.7 show the test setup.

Test date : 6^{th} Sept. 2012

Temperature : 26.26 ^{0}C

Relative Humidity : 81 %

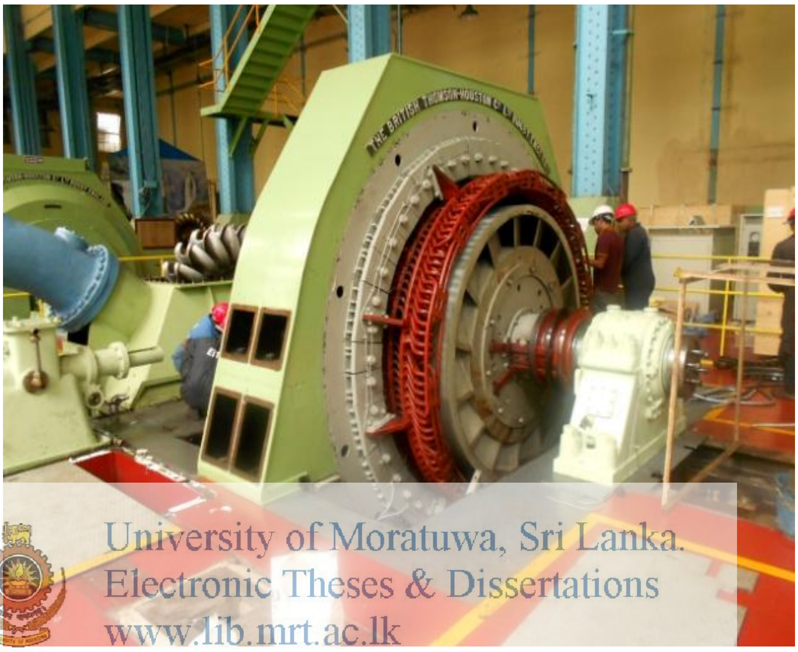

Figure 3.4 : VPI stator of Old Laxapana 'original in color'

Figure 3.5 : Setting up of the apparatus for DC ramp test 'original in color'

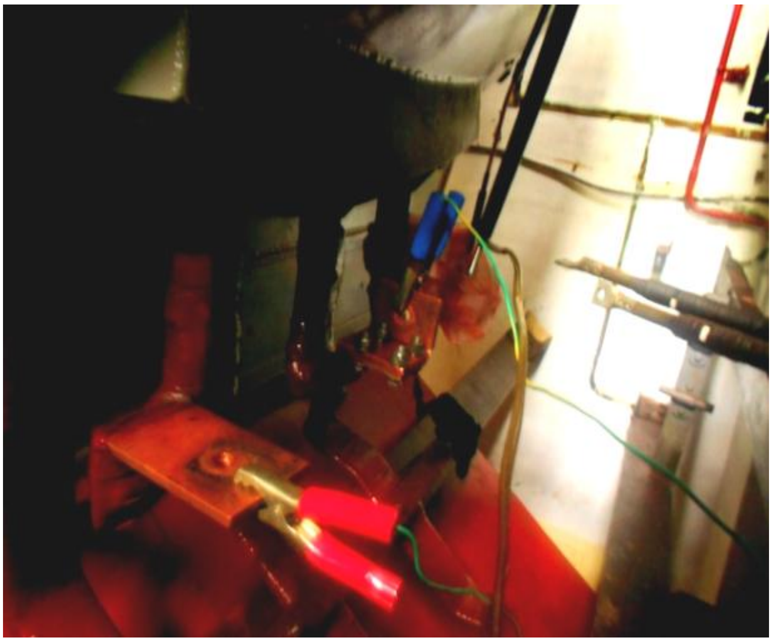

Figure 3.6 : Grounded two phases 'original in color'

Figure 3.7 : Real time plotting of I-V curve 'original in color'

3.1.4.2 Testing of Old Laxapana GVPI stator

Old laxapana newly installed GVPI stator was tested after six months in operation. After six months operation, the winding can be assumed as completely cured. Similar to the previous case, voltage was ramped at a rate of 1 kV/min up to 15 kV maximum. Current through the ground wall was measured. Figures 3.8, 3.9 and 3.10

show the test set up.

Test date : 1st March 2013

Temperature : 27.6 ^{0}C

Relative Humidity : 70.54%

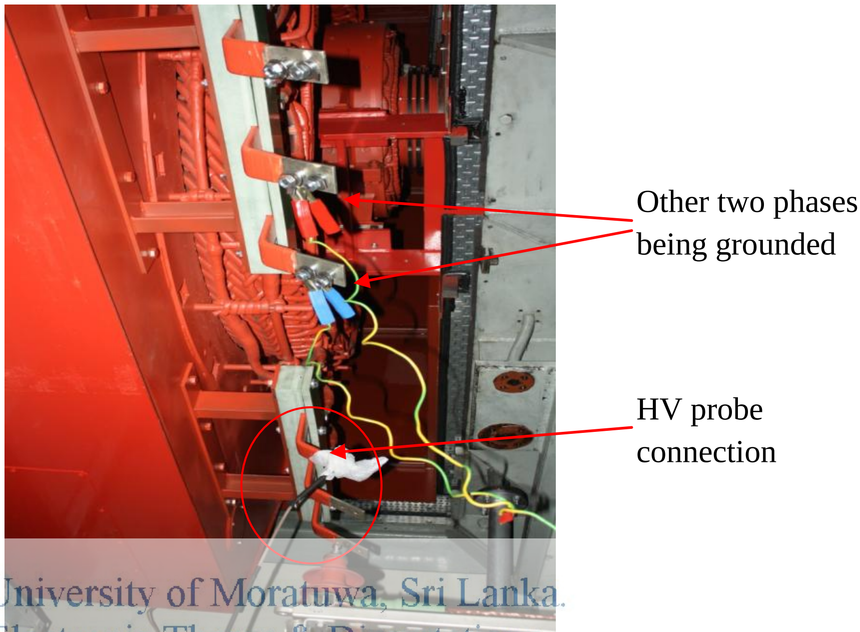

Figure 3.8 : High voltage connection and grounded two phases 'original in color'

Figure 3.9 : Setting up the apparatus to test GVPI stator 'original in color'

Figure 3.10 : Measurement of temperature and relative humidity 'original in color'

3.1.4.3 Testing of Wimalasurendra stator

Newly installed Wimalasurendra stator winding was tested after 3 months of operation. This time period can be assumed as sufficient for curing of the insulation. Voltage was ramped up at a rate of 1 kV/min up to 15 kV. Figure 3.11 show the winding and figure 3.12 show the test setup.

Test date : 22nd March 2013

Temperature : $28.7\ ^{0}C$

Relative Humidity : 55.5 %

Figure 3.11: Wimalasurendra form wound stator 'original in color'

Figure 3.12 : Applying high voltage through the DCR-50 instrument at Wimalasurendra power station 'original in color'

3.2 Frequency Domain Spectroscopy Test

Exposing the insulation to a wide band of frequency can reveal much more details about the insulation than the tests done at the power frequency. Effect of moisture and ionic compounds in the dielectric are more prominent in the low frequency region.

The dielectric response is measured from a three terminal method, where one is the output, the other is the measurement and the third is the guard terminal to avoid unnecessary disturbances.

In this test, generally 220V AC output voltage is applied to the isolated phase winding and the current through the groundwall is measured from the grounded stator frame. Other two phase windings are shorted and earthed and connected to the guard terminal to avoid the effect of those two phases to the measurement.

Test was carried out from the instrument ‘DIRANA’ which stands for the Dielectric Response Analyzer. Frequency sweep can be obtained in the range of 0.1 mHz -4 kHz from this instrument. Figure 3.13 shows the schematic of the test set-up.

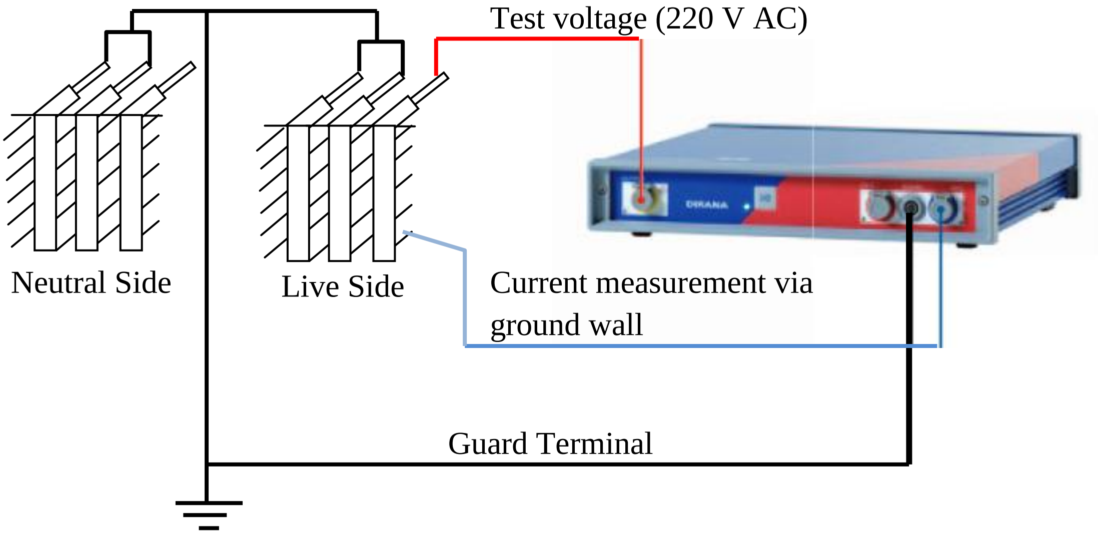

Figure 3.13 : Schematic diagram for frequency domain spectroscopy test set-up

3.2.1 Dielectric behavior along a frequency sweep

Polarization and dielectric losses are affected by parameters such as moisture content, contamination and temperature of the dielectric. These effects are different at different frequencies.

When alternating electric field of frequency (f) is applied to a dielectric material, polarization can only happen if the oscillation time of the applied field ($T=1/f$) is greater than the dipole relaxation time (τ). Then only the polarization process can be completely established. If the oscillation time of the field, T, is much smaller than the dipole relaxation time, τ, then polarization does not occur since the dipoles cannot respond to the rapid oscillations of the field. Then it ceases its contribution to the ε', which is relative permittivity of the material [5].

3.2.1.1 Complex permittivity

Dielectric losses occur due to resonance effect around a particular frequency. The complex permittivity is the term used to represent both the real and loss component of the dielectric. The complex permittivity (ε ∗) is given by the following formula, where ε' is the relative permittivity and ε'' is the dielectric loss.

$$\varepsilon * = \varepsilon' - j\varepsilon'' \quad (3.3)$$

Variation of *ε'* with the frequency is called the dispersion curve and typical dispersion curve for a dielectric is shown in figure 3.14 [5]. When the frequency is very large, the polarization does not exist. Then the relative permittivity is equal to the vacuum permittivity.

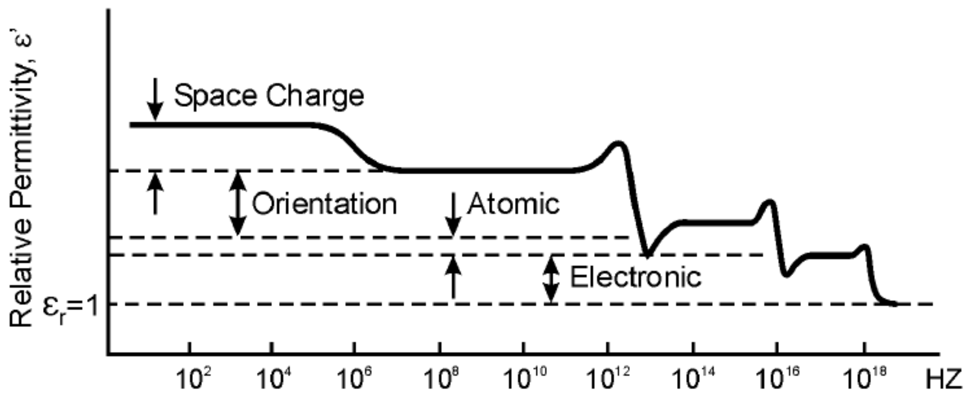

Figure 3.14 : Dispersion curve

Source: (L.M.Rux, "The physical phenomena associated with stator winding insulation condition as detected by the ramped direct high voltage method", Ph.D. dissertation, Dept.of Elect.Eng. ,Mississipi University, Mississipi state, Mississipi, 2004)

The ratio between the imaginary and real part of the complex permittivity is derived as loss tangent.

$$Tan\ \delta = \frac{\varepsilon''}{\varepsilon'} \qquad (3.4)$$

3.2.1.2 Relative permittivity (ε_r)

Relative permittivity (ε_r) is the same as the real part of permittivity (ε'). It is the dielectric permittivity of a material expressed as a ratio relative to the vacuum permittivity. It is also known as the dielectric constant.

$$\varepsilon_r(\omega) = \frac{\varepsilon\,(\omega)}{\varepsilon_0} \qquad (3.5)$$

Permittivity of free space is considered as 1. For all practical insulating materials ε_r is greater than unity. It relates to the charge displacement of polarization.

3.2.1.3 Dielectric loss

Dielectric losses are represented by the imaginary part of complex permittivity, ε''. It represents the dissipative effects of dielectric polarization. Smaller value of ε'' indicates the good quality of the insulation.

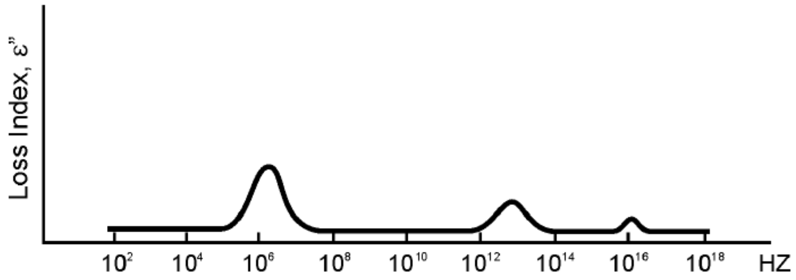

Figure 3.15 : Variation of loss index with frequency

Source: (L.M.Rux, "The physical phenomena associated with stator winding insulation condition as detected by the ramped direct high voltage method", Ph.D. dissertation, Dept.of Elect.Eng. ,Mississipi University, Mississipi state, Mississipi, 2004)

3.2.2 Site tests

Tests were carried out for the three specimens listed in table 3.1. Due to the high capacitance of the stator windings the test voltage and the frequency sweep range had to be limited. The inductance of the equipment was not sufficient to allow the large charging required by the stator winding. Summary of test conditions is given in table 3.2.

Table 3.2 : Test conditions

Winding	Insulation	Applied Voltage	Frequency range
Old Laxapana Unit 3 (before rehabilitation)	VPI	50 V	50 mHz-500 Hz
Old Laxapana Unit 1 (after rehabilitation)	GVPI	50 V	1 mHz-500 Hz
Wimalasurendra Unit 1 (after rehabilitation)	VPI	50 V	1mHz-200 Hz

3.2.2.1 FDS test for Old Laxapana VPI Stator

Test Date : 6th September 2012

Figure 3.16 : Voltage application to one phase of VPI stator of Old Laxapana while other two phases being guarded 'original in color'

3.2.2.2 FDS test for Old Laxapana GVPI Stator

Test Date: 2nd May 2014

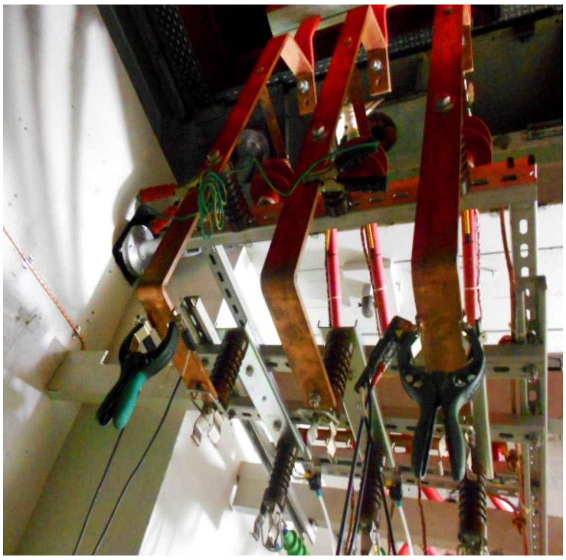

Figure 3.17 : Voltage application to one phase of GVPI stator while other two phases being guarded 'original in color'

3.2.2.3 FDS test for Wimalasurendra VPI Stator

Test Date: 31st December 2013

Figure 3.18 Monitoring the waveform along the frequency sweep 'original in color'

3.2.3 Behavior of dielectric with moisture

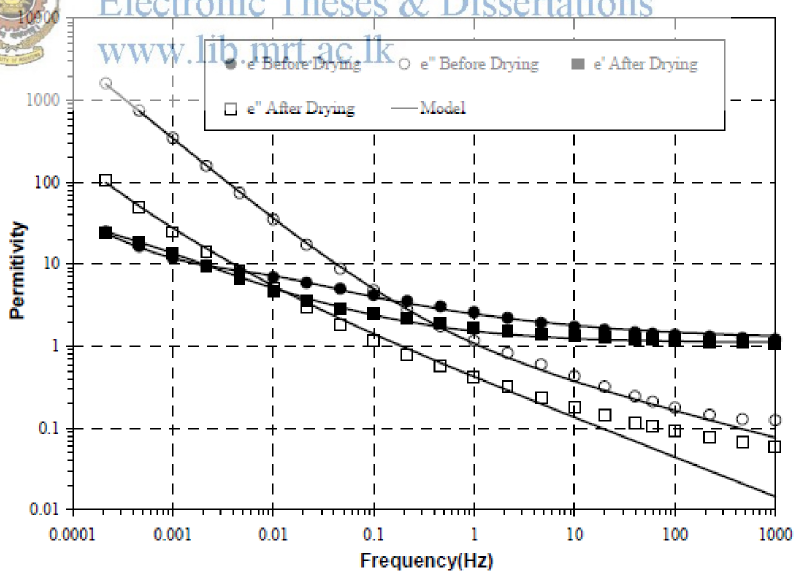

Figure 3.19 : Real and Imaginary parts of permittivity variation before and after drying for 48 hours

Source: (M.A.R.M. Fernando et. al., IEEE Transactions on Dielectrics and Electrical Insulation Vol. 20, No. 6, December, 2013)

Since international standards have not been established yet for assessing the dielectric spectroscopy, experience based assessment has to be carried out.

Fernando et al. in [19] has studied the variation of real and imaginary parts of permittivity and loss tangent of samples of generator windings along the frequency sweep with drying effect. From the experimental data of figure 3.19, it could be clearly identified that real part of permittivity (ε') and the losses (ε'') are significantly higher for the wet sample in the low frequency region.

Figure 3.20 show that loss tangent is higher for the samples with higher moisture contents in the low frequency region.

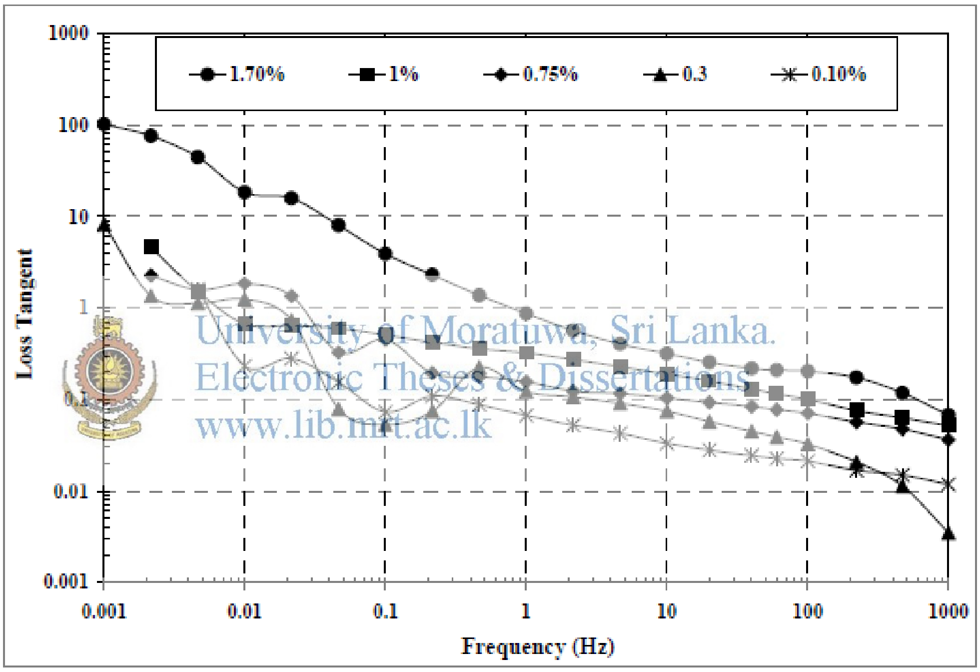

Figure 3.20 : Variation of loss tangent with different moisture contents at 70 ^{0}C

Source: (M.A.R.M.Fernando et.al. IEEE Transactions on Dielectrics and Electrical Insulation Vol. 20, No. 6, December, 2013)

4.1 Analysis by Observation on DC Ramp Test Results

Experienced evaluator can interpret the condition of the insulation system by analyzing the I-V curve obtained by the DC ramp test.

Test curves were analyzed by,

- Quantifying the magnitude of the measured current at 15 kV
- Quantifying the slope of the I-V response
- Quantifying the voltage at which the trace become non-linear

The I-V curve for R phase of Old Laxapana VPI Stator obtained from DC ramp test is shown in figure 4.1. Relevant measured data is given in table A.1 in appendix A.

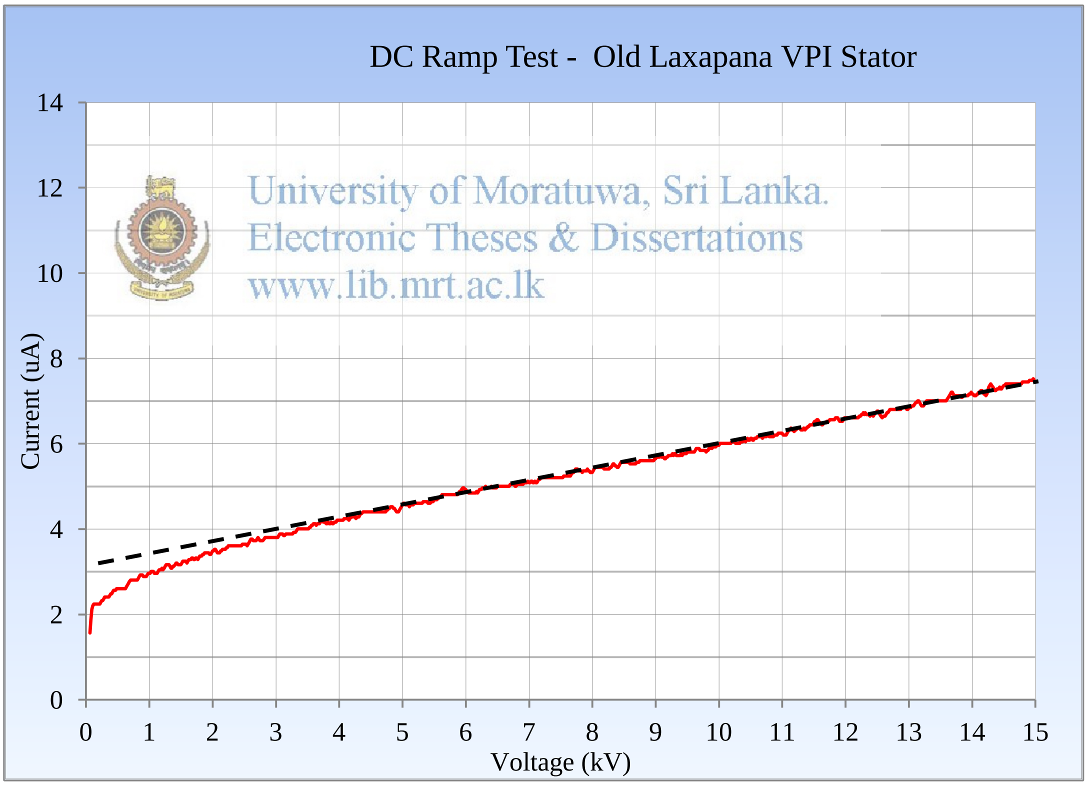

Figure 4.1 : Current vs. voltage plot for Old Laxapana VPI stator

Behavior of the I-V curve is very smooth and no indication of current spikes. Curve is linear over full range of voltage. No tape separation of the insulation. Current at 15 kV is 7.6 μA.

The I-V curve obtained for R phase of Old Laxapana newly installed GVPI stator is shown in figure 4.2 below. Actual measured data is given in table A.2 in appendix A.

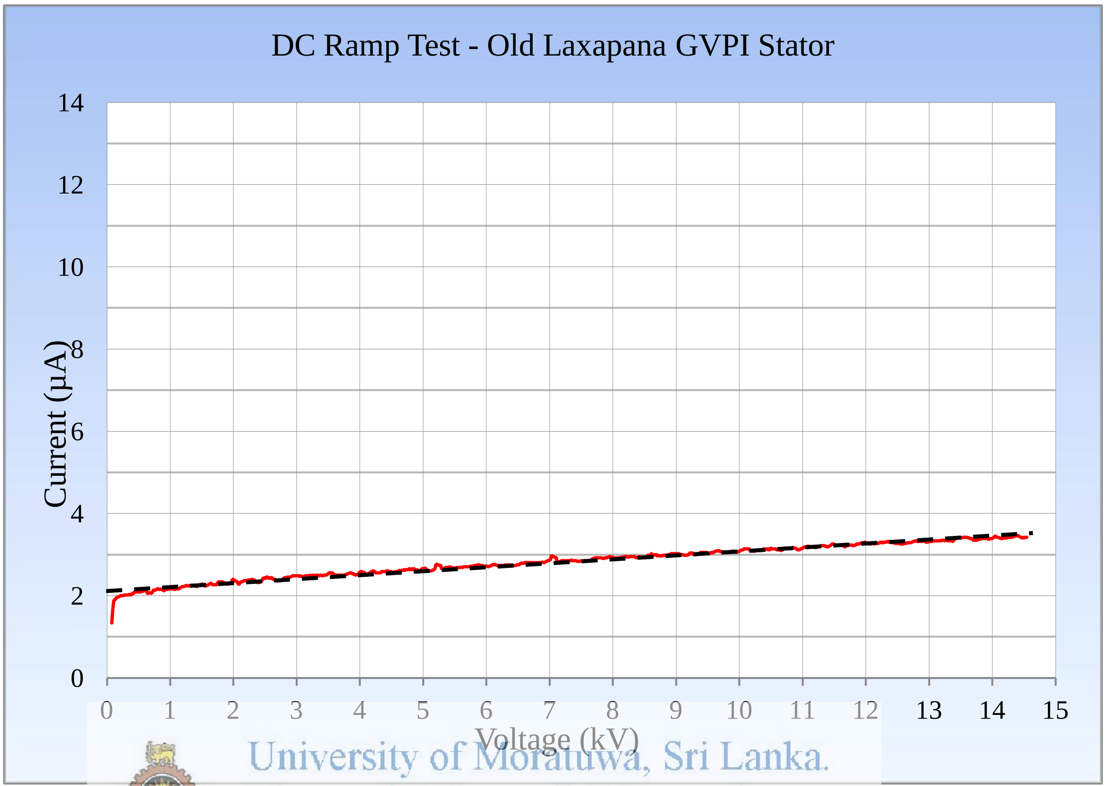

Figure 4.2 : Current vs. voltage plot for Old Laxapana GVPI stator

Linear rise of current with respect to the voltage is observed. No signs of winding delaminations. Curve is almost flat indicating minimum absorption and leakage. The leakage current at 15 kV is 3.5 µA which is relatively a very small value.

Figure 4.3 shows the I-V response curve for DC ramp test done for R phase of Wimalasurendra VPI Stator. Relevant measurements are given in table A.3 in appendix A.

Leakage current at 15 kV is 12.3 µA which is relatively high compared with the new GVPI insulation. As the voltage increases, current has increased linearly up to 12.2 kV, and afterwards has started rising non-linearly. This could be due to inadequate resin cure of the new epoxy mica stator. No signs of winding delaminations observed. Slope is higher compared to the GVPI insulation.

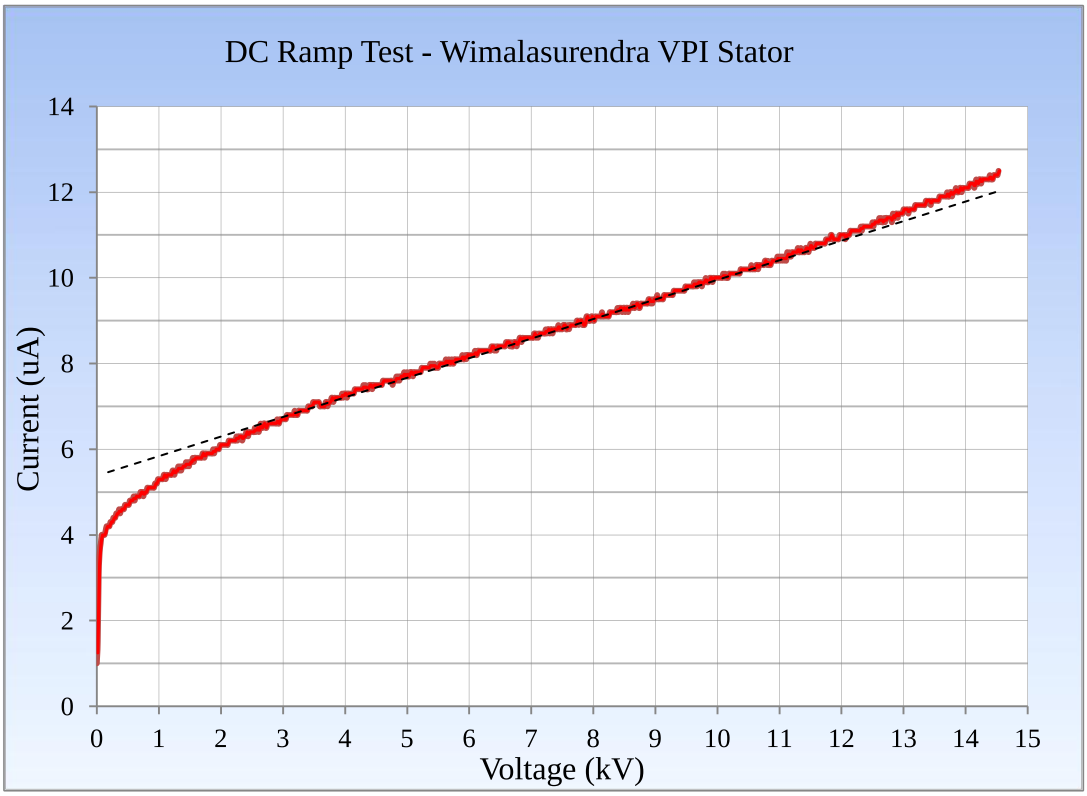

Figure 4.3 : Current vs. voltage plot for Wimalasurendra new VPI stator

Table 4.1 summarizes the observations on three stators.

Table 4.1 : Summary of observations from DC ramp test results

	OLPS VPI	OLPS GVPI	WPS VPI
Measured current at 15 kV	7.6 μA	3.5 μA	12.3 μA
Slope	0.3	0.09	0.44
Point at which curve become non linear	-	-	12.2 kV

The information available in table 4.1 shows that the slope of the I-V curve is significantly less in the GVPI insulation compared to the other two specimens. The slope of the curve is an indication of the polarization inside the dielectric. Hence the polarization is minimum in the new GVPI insulation which is a highly preferred quality for the insulation as low polarizable material has lesser tendency for moisture absorption.

4.2 Analysis Using a Mathematical Model for the DC Ramp Test Results

Abnormality observed in the I-V response curve of DC ramp test could be an indication of contamination caused by moisture absorption or material degrading with ageing, partial discharges between layers of delaminated insulation, dipole polarization due to inadequate resin cure, surface leakages or surface corona activity.

Analyzing by observing the behavior of the total current is not always accurate since it shows combined effect of capacitance charging, absorption and the leakage currents. It means the actual cause can be different than what is interpreted by observing the total current. Knowledge on high voltage insulation and previous diagnostic experience is required to accurately decide the condition of the insulation. In some cases the DC ramp test is performed and insulation condition is assessed as excellent by non-specialists.

Absorption current is the most significant current component in predicting the insulation condition of a dielectric. The chemical changes or deteriorations could be clearly identified by the absorption current component. The geometrical capacitance charging current is inherent to the physical dimensions of a winding, hence not considered in assessing the insulation condition. The leakage current component is due to impurities or contaminants but not attributed to the basic substance. Hence a mathematical model was used in this study to separate the absorption current component in order to interpret the condition of the insulation.

4.3 Mathematical Model

According to the Maxwell's equations, when a linear dielectric material is subjected to an arbitrarily time varying electric field, the total current density through the dielectric material is given by,

$$J(t) = \nabla \wedge H(t) = \sigma E(t) + \frac{\partial}{\partial t}[\epsilon_0 E(t) + P(t)] \quad (4.1)$$

Where,

J (t) - Current density

H - Magnetic Field

σ	-	Material conductivity
E (t)	-	Arbitrarily varying electric field
ε_0	-	Permittivity of the vacuum
P (t)	-	Time dependant polarization

The first term of equation 4.1 represents leakage current; second term capacitive charging current and the third term absorption current respectively.

P(t) denotes the polarization with its rapid and slow phenomena,

$$P(t) = \varepsilon_0 (\varepsilon_\infty - 1)E(t) + \varepsilon_0 \int_0^t f(\tau)E(t-\tau)d\tau \qquad (4.2)$$

Where,

f (τ)	-	Response function of the material
ϵ_∞	-	High frequency permittivity

By combining equation 4.1 and 4.2, the current density can be written as

$$J(t) = \sigma E(t) + \epsilon_0 \frac{\partial}{\partial t}\left[\epsilon_\infty E(t) + \int_0^t f(\tau)E(t-\tau)d\tau\right] \qquad (4.3)$$

When Voltage U (t) is applied,

$$I(t) = \frac{C_0\,\sigma U(t)}{\epsilon_0} + C_0 \frac{\partial}{\partial t}\left[\epsilon_\infty U(t) + \int_0^t f\,(\tau)U(t-\tau)d\tau\right] \qquad (4.4)$$

When the applied voltage is U (t)= αt ,

Capacitive current and leakage current can be approximated as,

$$I_{leakage} \approx \frac{C_0 \sigma \alpha t}{\varepsilon_0} \approx \frac{\alpha t}{R} \qquad (4.5)$$

$$I_{cap} \approx c_0 \varepsilon_\infty \alpha \approx C_\infty \alpha \qquad (4.6)$$

$$(\sigma = \frac{1}{\rho} \;\; and \;\rho = \frac{RA}{l})$$

Where

R	-	Resistance for leakage current
C_∞	-	Capacitance at higher frequencies

By assuming that the response function of the insulation follows Curie-Von Schweidler behaviour (i.e. f (t) = At^{-n}) the absorption current can be approximated as follows [19]. A and n are parameters relative to the insulation system.

$$I_{abs} \approx (\frac{\alpha C_0 A t^{1-n}}{(1-n)}) \tag{4.7}$$

Substituting $C_0 = \frac{C_\infty}{\varepsilon_\infty}$,

$$I_{abs} \approx \frac{\alpha K C_\infty \ t^{(1-n)}}{(1-n)} \tag{4.8}$$

where $K = \frac{A}{\varepsilon_\infty}$

Now the resultant current in DC ramp test can be written as,

$$I(t) = \alpha[\frac{t}{R} + C_\infty + \frac{K C_\infty}{(1-n)} t^{1-n}] \tag{4.9}$$

Since the applied ramp rate is 1 kV/min,

$$\alpha = \frac{1000\ V}{60\ s} = 16.67\ V/s$$

C_∞ Values measured from the FDS tests shown in table 4.2 were substituted in equation 4.9.

Table 4.2 : Capacitance at higher frequencies

	OPLS VPI	OLPS GVPI	WPS VPI
High frequency capacitance (C_∞)	91 nF	110 nF	158 nF

Using the curve fitting method in MATLAB software R, K and n were varied in order to obtain the best fit. Ranges for those parameters were bounded to the realistic values.

As depicted by the figures in table 4.3, the accuracy of the best fit was maintained such that R-Square value was always greater than 0.85.

Using the best fit parameters, the capacitive, leakage and polarization current

Components were separated for carrying out a better analysis.

Table 4.3 : Statistics of goodness of fit

	OLPS VPI	OLPS GVPI	WPS VPI
SSE	9.946	5.866	18.65
R-Square	0.9947	0.8677	0.9957
Adjusted R-square	0.9947	0.8665	0.9957
RMSE	0.1019	0.1594	0.1418

Screen prints of MATLAB workspace is attached in Appendix B.

4.4 Current component separation

Applying the estimated parameters again to the mathematical model, the capacitive, leakage and absorption current components were re-calculated. Behavior of absorption current is clearly observed in Figures 4.4, 4.5 and 4.6.

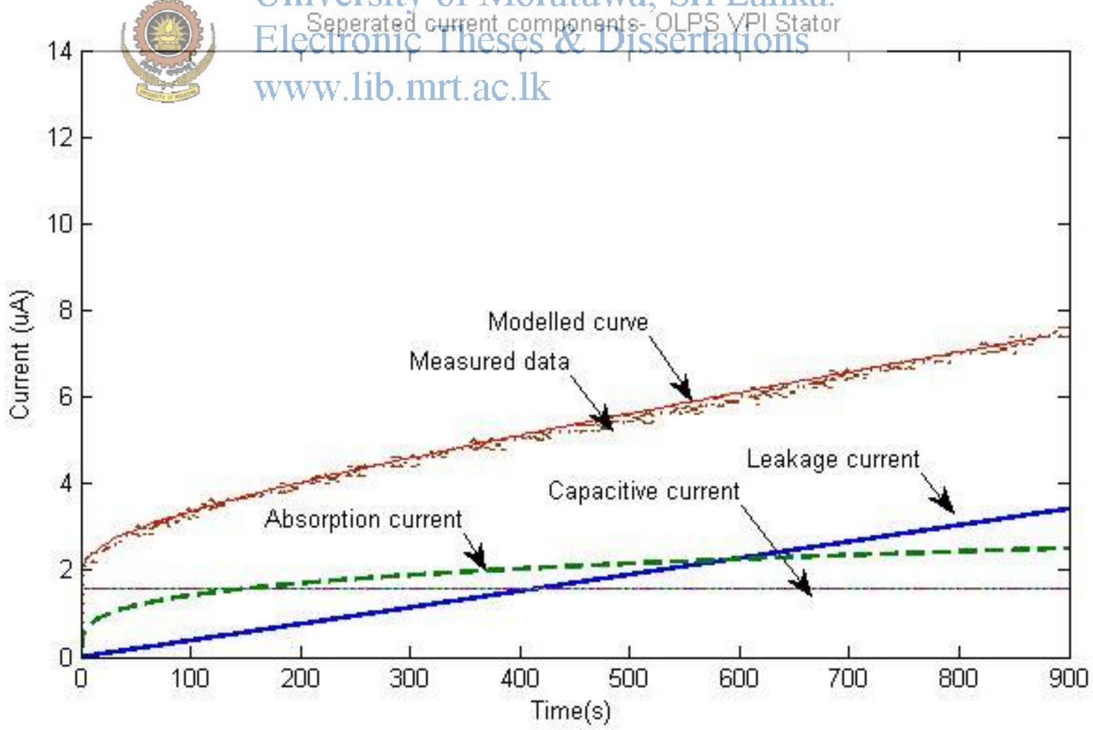

Figure 4.4 : Separated current components of DC ramp test- OLPS VPI stator

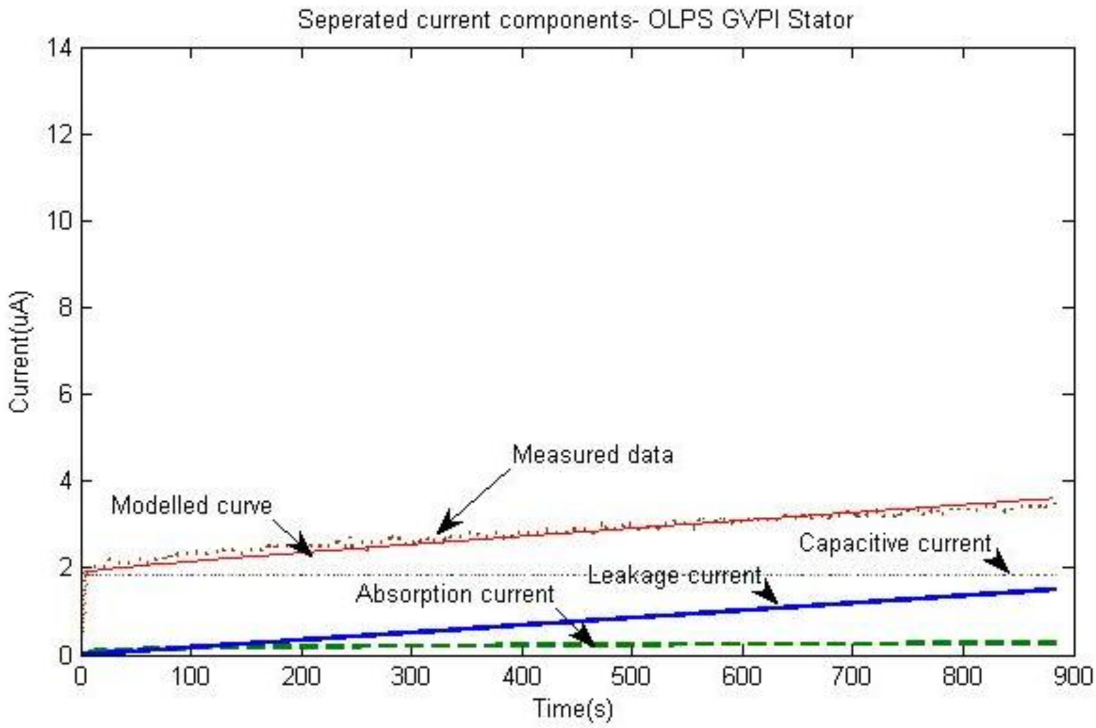

Figure 4.5 : Separated current components of DC ramp test - OLPS GVPI stator

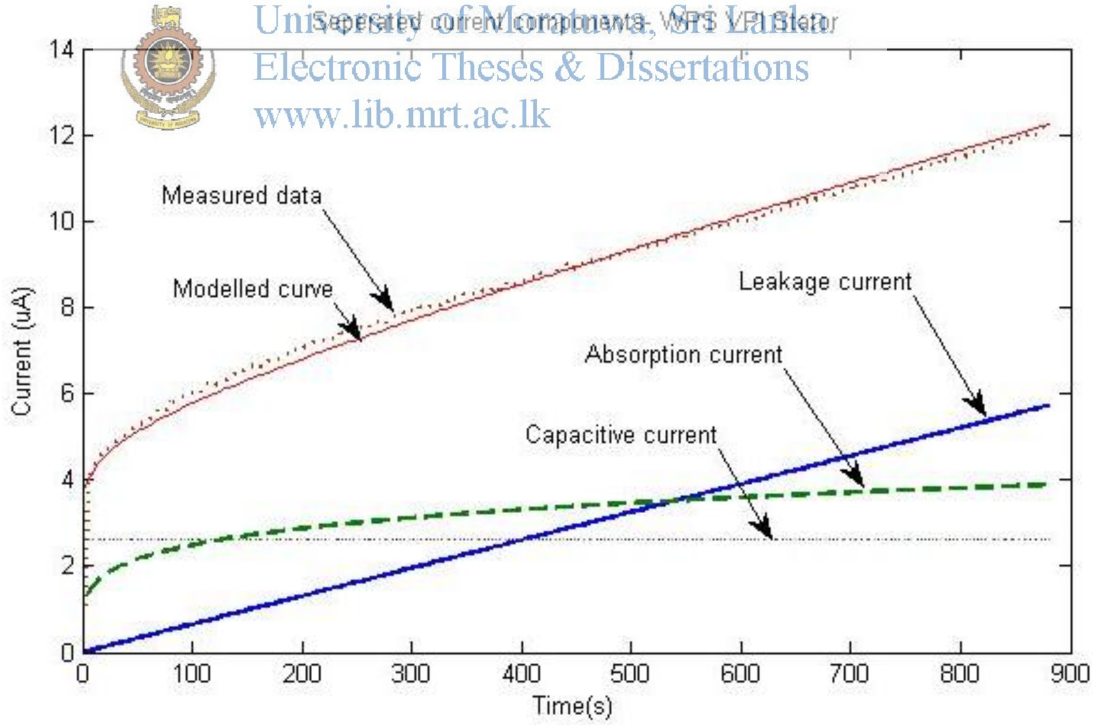

Figure 4.6 : Separated current components of DC ramp test- WPS VPI stator

The modeled curve gives close approximation to the measured data.

Table 4.4 summarizes the absorption currents at 15 kV for the three specimens.

Table 4.4 : Information obtained from parameter estimation

	OLPS VPI Stator	OLPS GVPI Stator	WPS VPI Stator
Absorption current at 15 kV	2.51 µA	0.27 µA	3.88 µA
Absorption current at 15kV as % of total measured current	33%	7.7%	31.5%

Significantly less absorption current, which contributes only for 7.7% of the total measured current, is observed for the new GVPI insulation. Other two VPI insulations demonstrated more than four times higher absorption currents compared to GVPI insulation. Increase of the absorption current over the voltage is also very small for GVPI insulation. It indicates that none of ageing of material or adhesives, oxidation ageing, thermal ageing or byproducts of partial discharges exists in the insulation. This result gives a clear indication that insulation properties of GVPI insulation are superior.

4.5 Analysis on Frequency Domain Spectroscopy Test Results

A single diagnostic test is not suited to detect the root cause of stator winding insulation problems. Therefore Frequency domain Spectroscopy test was also utilized for confirmation of the results. Figure 4.7 , figure 4.8 and figure 4.9 demonstrates the behavior of the real part of the permittivity, imaginary part of the permittivity, and dissipation factor along the frequency sweep relatively. The relevant measurements are given in table A.4, table A.5 and table A.6 in appendix A.

The effect of polarization activities are prominent in the low frequency region since there is sufficient time for the dielectric materials to align according to the electric field which is changing at a slower phase. Hence the behavior of electrical parameters such as real and imaginary part of permittivity and dissipation factor in the low frequency region can provide valuable information about the condition of the insulation.

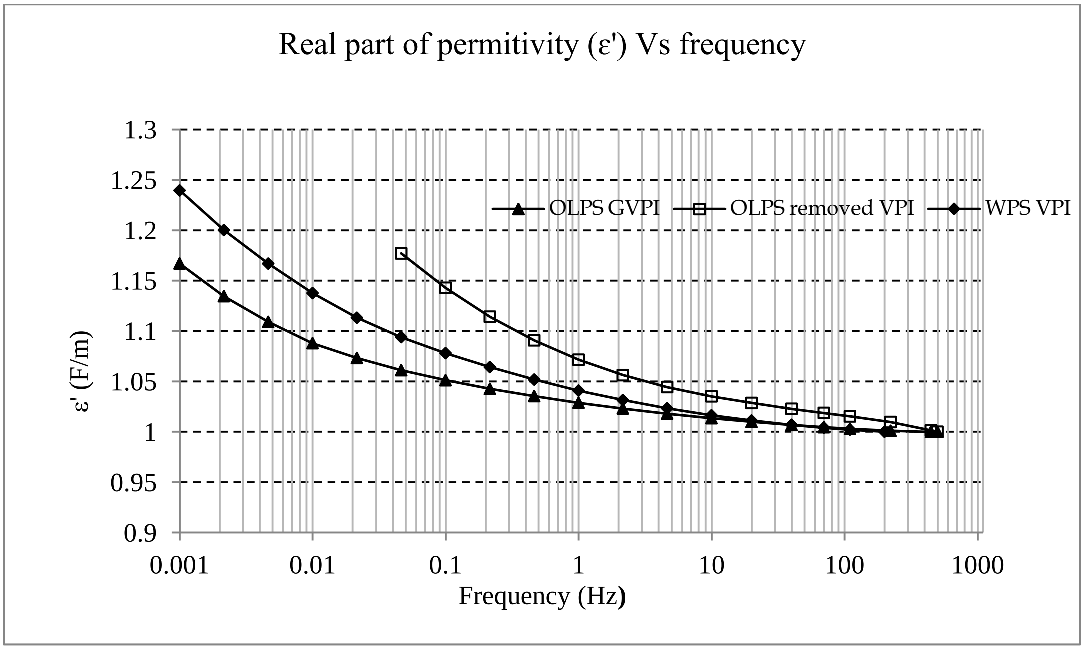

Figure 4.7 : Real part of permittivity vs frequency plot

The three specimens made of Epoxy Mica material should inherit similar relative permittivity values in an ideal case. Although the absolute values may have errors due to inherent errors of the instrument, the relative values provide very clear cross comparison. The changes observed in relative permittivity depict the influence of contaminations mainly due to moisture ingress. By observing the behavior of the relative permittivity in the low frequency region (i.e. 1 mHz- 1 Hz), it is understood that the minimum moisture absorption is in the new GVPI insulation. The Wimalasurendra VPI insulation shows little higher tendency of moisture absorption and the old VPI stator shows highest moisture ingress.

Variation of the imaginary part of the permittivity (ε'') along the frequency sweep is observed from figure 4.8 below. The imaginary part of the permittivity represents the dielectric losses. Lowest ε'' values are observed for the new GVPI insulation in low frequency region and highest ε'' values are observed for the old VPI insulation. The new VPI insulation of Wimalasurendra shows moderate ε'' values.

Dissipation factor is one electrical parameter that represents the losses in a dielectric medium. The information revealed from figure 4.8 is further verified by observing the dissipation factor Vs frequency plot in figure 4.9.

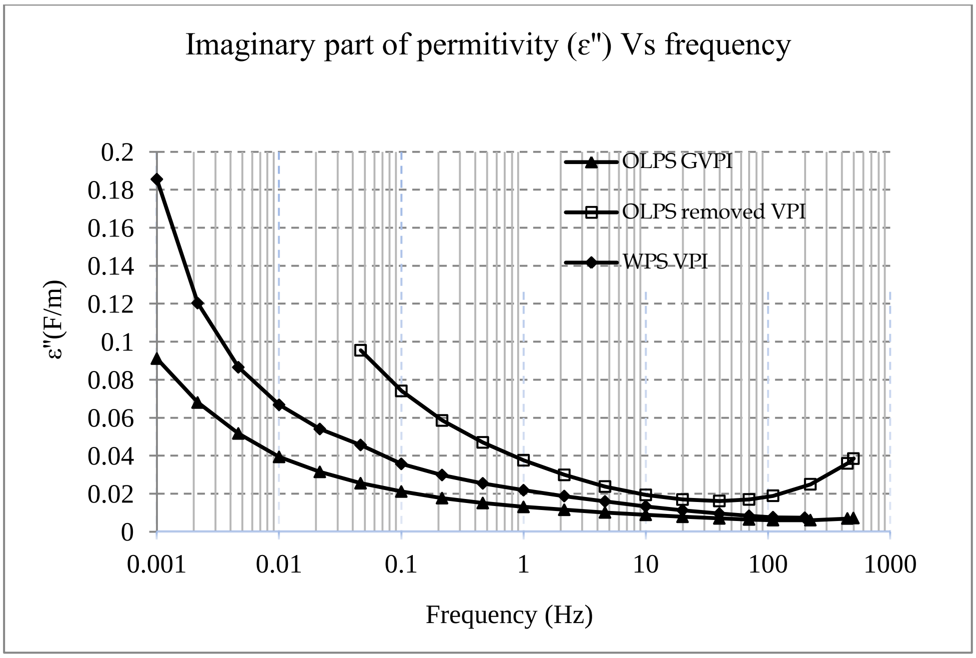

Figure 4.8 : Imaginary part of permittivity vs frequency plot

It is observed that the lowest dissipation factor in the low frequency region exists in the new GVPI insulation. Old VPI insulation has higher dissipation factor in the low frequency region implying the aged Class F insulation is highly wet than new VPI and GVPI insulation. The new VPI insulation of Wimalasurendra power station demonstrates moderately wet condition.

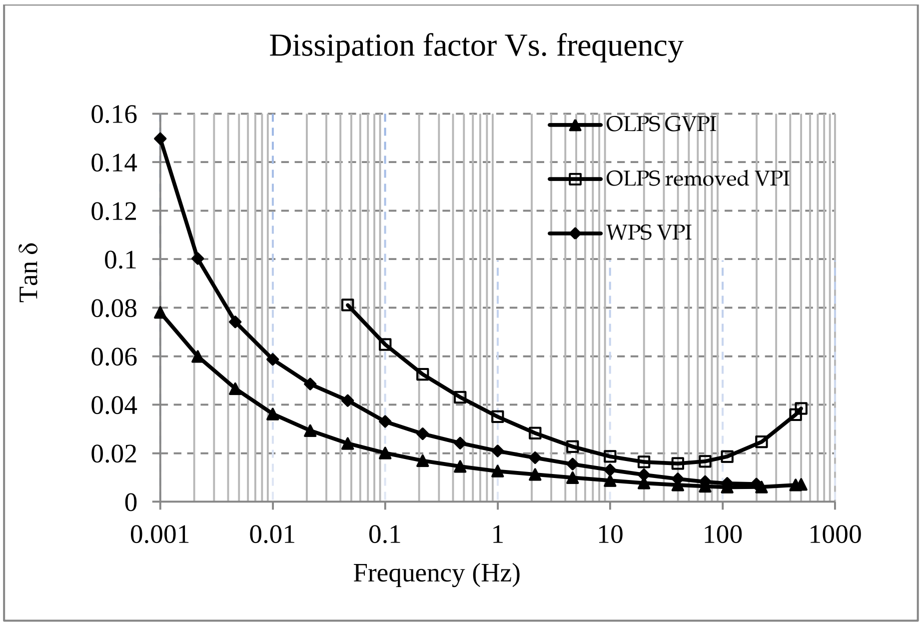

Figure 4.9 : Dissipation factor vs frequency plot

The dissipation factors at 50 Hz are measured during the FDS test is shown in table 4.5 below.

Table 4.5 : Dissipation factor at power frequency

Specimen	OLPS VPI	OLPS GVPI	WPS VPI
Dissipation factor(50 Hz)	0.016	0.006	0.008

The dissipation factor at power frequency, which is an indication of thermal conductivity, does not show significant difference, but in order to observe the real condition of the insulation, the low frequency region should be analysed.

5. CONCLUSION

5.1 Conclusion

The principal goal of this research was to assess the condition of the global vacuum pressure impregnation insulation of the newly installed stator winding of Old Laxapana power station after the rehabilitation project, in comparison with the vacuum pressure impregnation insulation used in old stator which was in operation for 33 years prior to the rehabilitation. Some premature failures of global vacuum pressure impregnated stators that has been reported worldwide influenced to proceed with this type of comparative assessment. Since the two samples were not of the same age, newly installed vacuum pressure impregnated stator of Wimalasurendra power station was also used as a test specimen to represent the new condition of VPI insulation. The latter is of the same rated voltage (i.e. 11 kV) and same winding construction method (form wound multi turn coils) as Old Laxapana stators.

A thorough literature study was carried out on stator insulation. It included identifying main segments of stator insulation, such as strand insulation, turn insulation, groundwall insulation, semi conductive corona protection and end corona protection. Also the evolution of insulating materials starting from Asphalt Mica, Polyester Mica, and Epoxy resin to modern resins was studied with special attention to their salient features as dielectrics.

Two diagnostic tests, namely DC ramped voltage test and frequency domain spectroscopy test were utilized for the assessment. Both the tests are offline tests. Hence special permissions were obtained to stop the running generators to carry out the tests. Test instruments belonging to Asset Management branches of Ceylon Electricity Board were used.

Condition of the stator insulation is normally interpreted by observing the measured current response during dc ramp high-voltage testing. The ramped voltage test curves were analyzed by quantifying the magnitude of the measured current at 15 kV, the slope of the I-V response, and by noting the voltage at which the trace becomes nonlinear. Minimum slope and minimum current at 15 kV was observed for the

GVPI insulation. The trace was linear until 15 kV. In overall, it showed features of very high quality insulation.

The interpretations on measured current of DC ramp test are not always accurate since the interpreter can only see the total measured current which is the combined effect of capacitive charging, absorption and leakage currents but not the individual effect of those currents. Therefore theoretical explanation was used for separating these current components for better analysis. This theoretical approach adopted is a method well established by many research done locally and worldwide.

Applying the mathematical model to the measured data in the Matlab software, the best fit curve was obtained and the capacitive, absorption and leakage currents were separated. The main objective of the modeling was to sort out the absorption current component which is very significant in determining the insulation quality. The rate of rise of absorption current with respect to the voltage is also one important feature which reveals insulation quality. In order to compare the absorption currents among the stators of different capacity, absorption current was calculated as a percentage of total measured current. It could be clearly observed that the new GVPI insulation has minimum absorption current and negligible rise with the voltage. The other two VPI stators exhibited relatively higher absorption currents; nearly four times larger than that of the GVPI stator.

Frequency domain spectroscopy test is found to be informative presenting individual relative and imaginary components of permittivity and dissipation factor and measuring these properties over a wide range of frequency. The greatest difference among the test specimens were observed at the lowest frequencies, where polarization effects have more time to react to the changing electric field. But this method has not very commonly been used on rotating machine insulation; hence no guidelines exist for determining typical versus abnormal deviations. Therefore pervious research results obtained for variations in these parameters with drying and wetting effects were used to analyze the curves.

The lowest relative and imaginary components of permittivity were observed for the GVPI insulation in the low frequency region indicating the minimum moisture absorption and dielectric losses respectively. Lowest dissipation factor was observed for the GVPI insulation in the low frequency region re-confirming high quality of insulation with minimum dielectric losses.

When comparing the two VPI stators, the Old VPI stator demonstrated high values of real and imaginary parts of the permittivity in the low frequency region indicating moisture ingress condition of the insulation and higher dielectric losses. The dissipation factor of new VPI insulation was lower compared to the old VPI insulation. It indicates the new VPI insulation has better performances compared to the Old VPI stator but both VPI stators are out rated by the performance of the high quality GVPI stator insulation.

5.2 Recommendations

This study has well proven the superior insulation qualities of the GVPI insulation over VPI insulation. Hence, based on this study it could be recommended to adopt GVPI insulation methodology for all small and micro hydro generators to be installed in Sri Lanka in future time. Generators of GVPI insulation can be recommended for upcoming 2 x 17.5 MW Broadlands and 2 x 15.5 MW Moragolla hydro power plants. This will bring down the high costs while rendering high quality of insulation. The buyers should request to perform DC ramp test and FDS tests at factory to evaluate the quality of the workmanship and material. More stringent ways of interpreting the DC ramp test such as current component separation should be used for analysis.

References

[1] R. Brutsch, M. Tari, K. Frohlich, T. Weiers, and R. Vogelsang,"Insulation failure mechanisms of power generators", IEEE Electr.Insul. Magazine, Vol. 24, No. 4, pp. 17-25, 2008.

[2] CIGRE Study Committee SC11, EG11.02, "Hydro-generator Failures– Results of the Survey," 2003.

[3] Greg C. Stone et al.,"Rotating Machine Insulation Systems", in *Electrical Insulation for rotating machines Design, Evaluation, Aging, Testing & Repair,* New Jersy, John Wily and Sons Inc., 2004, Ch.1, pp 9-31

[4] Greg C. Stone et al.,"Historical Development of Insulation Materials and Systems", in *Electrical Insulation for rotating machines Design, Evaluation, Aging, Testing & Repair,* New Jersy, John Wily and Sons Inc., 2004, Ch.3, pp 74-92

[5] L.M.Rux, "The physical phenomena associated with stator winding insulation condition as detected by the ramped direct high voltage method", Ph.D. dissertation, Dept.of Elect.Eng. ,Mississipi University, Mississipi state, Mississipi, 2004.

[6] A. Nakayama, K Haga and S. Inoue., "Development of Global Vacuum Pressure Impregnation Insulation system for Turbine Generators", Proc. 2000 World Geothermal Congress, Kyushu - Tohoku, Japan

[7] G.C.Stone. (2010, August 4).*Success of Rewinds of GVPI stators*. [Online Forum]. Available at http://www.generatortechnicalforum.org/portal/forum/ viewthread.php?Thread_id=40&fgroup=1#post_86

[8] G. C. Stone et al., "Recent problems experienced with motor and generator windings",in *Institute of Electrical and Electronic Engineers Petroleum and Chemical Industry Technical Conf.* ,Anaheim, California,USA, 2009

[9] Stefanos Diamantis.(2010,September 4). *Success of Rewinds of GVPI stators*. [Online Forum] Available at, http://www.generatortechnicalforum.org/portal/forum/ viewthread.php?thread_id=40&fgroup=1#post_86

[10] Clyde V Maughan. (2010, September 4). *Success of Rewinds of GVPI stators***.** [On line Forum]. Available at http://www.generatortechnicalforum.org/portal/forum/ viewthread.php?thread_id=40&fgroup=1#post_86

[11] Padma Kumar. (2010, June 22).*Damage in GVPI stator*. [Online Forum] Available at http://www.generatortechnicalforum.org/portal/forum/viewthread.php? thread_id=478&fgroup=1

[12] I.Rendroyoko, S. P. Handojo, D.S.Irawan , "Partial rewinding of 5 MW vacuum pressure impregnation (VPI) Generator winding", *Association of the Electricity Supply Industry of the East Asia and the West Pasific Conf. of the Electric Supply Industry Area II: Power Generation & Distributed Energy-9*,Taipei,Taiwan,2010

[13] D.G. Morrison, "Experience with Modern Air-Cooled Generator Stator Windings", in *Electric Power Research Institute Conf. on Electric Generator Predictive Maintenance and Refurbishment*", Tampa, 2003.

[14] B. Moore, D.Bucklew and P.Chantu, "Rewind of a Global VPI Repair", in *Conf. on On line Monitoting of Electrical Assets 2014*, Austin, Texas, 2014

[15]C. Maughan, *Resin Injection of Global VPI Generators*. [On line forum] 2010, Available at http://www.generatortechnicalforum.org/portal/forum/viewthread.php?thread_id=48&fgroup=1

[16] *Rotating Electrical Machines, Part-1 Rating and Performance*, IEC Standard 60034-1, 1999.

[17] *IEEE Recommended Practice for Insulation Testing of AC Electric Machinery (2300 V and Above) with High Direct Voltage*, IEEE Standard 95, 2002

[18] Lori Rux, Bill McDermid, "Assesing the condition of Hydro-generator stator widing insulation using the Ramped High Direct Voltage test Method", Institute of Electrical and Electronic Engineers Electrical Insulation Magazine, 2001,Vol.17,No.08

[19]M.A.R.M., Fernando et al., "Condition Assessment of Stator Insulation during Drying, Wetting and Electrical Ageing", *Institute of Electrical and Electronic Engineers Transactions on Dielectrics and Electrical Insulation*, 2013, Vol. 20, No. 6

Appendix-A

Table A.1: Current Vs Voltage measurement data for VPI stator of Old Laxapana

V(kV)	I(μA)	V(kV)	I((μA)	V(kV)	I((μA)	V(kV)	I((μA)
0.02	0.6	2.56	3.8	5.09	4.6	7.65	5.4
0.095	2.2	2.62	3.6	5.16	4.6	7.71	5.4
0.12	2.2	2.685	3.8	5.21	4.6	7.76	5.4
0.205	2.4	2.73	3.6	5.285	4.6	7.82	5.4
0.24	2.4	2.815	3.8	5.345	4.6	7.87	5.2
0.315	2.4	2.84	3.8	5.395	4.6	7.97	5.4
0.39	2.6	2.925	3.8	5.455	4.8	8.02	5.4
0.46	2.6	2.99	3.8	5.525	4.8	8.09	5.4
0.5	2.6	3.05	4	5.6	4.8	8.125	5.4
0.57	2.6	3.1	3.8	5.635	4.8	8.2	5.4
0.645	2.6	3.16	3.8	5.71	4.8	8.25	5.6
0.695	2.8	3.21	3.8	5.785	4.8	8.335	5.4
0.765	2.8	3.28	4	5.83	4.8	8.395	5.6
0.815	2.8	3.355	4	5.905	5	8.47	5.6
0.865	2.8	3.415	4	5.94	4.8	8.505	5.6
0.95	3	3.475	4	6.015	4.8	8.58	5.4
1	3	3.54	4.2	6.075	4.8	8.63	5.6
1.06	3	3.61	4	6.14	4.8	8.7	5.6
1.135	3	3.645	4.2	6.225	5	8.76	5.6
1.18	3	3.72	4	6.27	5	8.8	5.6
1.255	3.2	3.78	4.2	6.335	5	8.885	5.6
1.315	3.2	3.845	4.2	6.38	5	8.945	5.6
1.365	3.2	3.905	4.2	6.455	5	9.02	5.8
1.44	3.2	3.99	4.2	6.515	5	9.065	5.6
1.475	3.2	4.025	4.2	6.575	5	9.115	5.6
1.56	3.2	4.1	4.2	6.65	5	9.2	5.8
1.62	3.4	4.16	4.4	6.71	5	9.25	5.8
1.68	3.4	4.22	4.2	6.75	5.2	9.31	5.8
1.73	3.4	4.28	4.4	6.835	5	9.395	5.8
1.805	3.4	4.345	4.4	6.895	5	9.445	5.8
1.875	3.6	4.39	4.4	6.955	5	9.495	5.8
1.94	3.4	4.465	4.4	7.015	5	9.58	6
2	3.6	4.54	4.4	7.065	5.2	9.64	5.8
2.05	3.4	4.6	4.4	7.125	5.2	9.7	5.8
2.11	3.6	4.65	4.4	7.2	5.2	9.75	6
2.185	3.6	4.71	4.6	7.275	5.2	9.8	6
2.23	3.6	4.77	4.6	7.32	5.2	9.86	5.8
2.305	3.6	4.845	4.4	7.395	5.2	9.935	6
2.38	3.6	4.895	4.4	7.455	5.2	10.005	6
2.425	3.6	4.965	4.6	7.515	5.2	10.07	6
2.475	3.6	5.015	4.6	7.565	5.4	10.14	6

Table A.1: Current Vs. Voltage measurement data for VPI stator of Old Laxapana

V(kV)	I(μA)
10.19	6
10.25	6
10.31	6
10.385	6.2
10.445	6.2
10.495	6.2
10.57	6
10.63	6
10.69	6.2
10.75	6.2
10.8	6.2
10.9	6.4
10.935	6.2
10.995	6.2
11.055	6.2
11.12	6.2
11.19	6.4
11.265	6.4
11.315	6.4
11.375	6.4
11.435	6.6
11.51	6.6
11.57	6.4
11.62	6.4
11.68	6.6
11.74	6.6
11.8	6.6
11.865	6.6
11.925	6.6
11.995	6.6
12.045	6.6
12.12	6.6
12.18	6.8
12.255	6.8
12.315	6.6
12.375	6.6
12.45	6.8
12.51	6.6
12.535	6.6
12.605	6.8
12.68	6.8

V(kV)	I(μA)
12.755	6.8
12.79	6.8
12.875	6.8
12.915	7
12.985	6.8
13.06	7
13.11	6.8
13.18	7
13.255	7
13.315	7
13.39	7
13.435	7
13.475	7
13.56	7.2
13.62	7.2
13.68	7.2
13.745	7.2
13.79	7
13.865	7.2
13.925	7
13.975	7.2
14.05	7.2
14.11	7
14.17	7.4
14.245	7.2
14.305	7.4
14.365	7.4
14.425	7.4
14.485	7.4
14.56	7.4
14.62	7.4
14.66	7.4
14.73	7.4
14.815	7.6
14.855	7.4
14.915	7.4
14.99	7.6
15.035	7.6

Table A.2: Current Vs. Voltage measurement for Old Laxapana GVPI stator

V(kV)	I(μA)	V(kV)	I(μA)	V(kV)	I(μA)	V(kV)	I(μA)
0.01	0.1	2.61	2.4	5.21	2.6	7.785	2.9
0.085	1.8	2.67	2.3	5.26	2.7	7.885	3
0.145	1.9	2.73	2.4	5.31	2.6	7.91	2.9
0.195	2	2.795	2.4	5.395	2.7	7.97	3
0.255	2	2.84	2.5	5.455	2.7	8.04	2.9
0.29	2	2.925	2.4	5.525	2.6	8.115	2.9
0.375	2	2.965	2.5	5.59	2.7	8.19	3
0.435	2.2	3.05	2.5	5.635	2.7	8.215	2.9
0.52	2.1	3.11	2.5	5.725	2.7	8.3	3
0.585	2.1	3.195	2.4	5.77	2.7	8.345	3
0.63	2.1	3.22	2.5	5.83	2.8	8.42	2.9
0.72	2.1	3.32	2.5	5.905	2.8	8.47	2.9
0.765	2.1	3.355	2.6	5.955	2.7	8.54	2.9
0.83	2.2	3.415	2.5	6.03	2.8	8.65	3
0.9	2.2	3.475	2.5	6.075	2.7	8.65	3
0.975	2.2	3.56	2.6	6.14	2.7	8.725	2.9
1.01	2.1	3.61	2.5	6.21	2.8	8.775	3
1.11	2.1	3.685	2.5	6.295	2.8	8.86	3
1.145	2.2	3.755	2.5	6.335	2.7	8.92	3
1.205	2.3	3.83	2.5	6.395	2.7	8.995	3.1
1.265	2.2	3.88	2.6	6.465	2.8	9.08	3
1.33	2.3	3.94	2.5	6.53	2.7	9.13	3
1.375	2.2	4	2.5	6.6	2.8	9.175	3
1.475	2.3	4.06	2.7	6.64	2.8	9.265	2.9
1.51	2.3	4.11	2.5	6.7	2.8	9.335	3.1
1.61	2.3	4.21	2.6	6.81	2.8	9.375	3
1.66	2.3	4.27	2.6	6.845	2.8	9.435	3.1
1.705	2.3	4.33	2.4	6.905	2.8	9.47	3
1.78	2.4	4.37	2.6	6.955	2.8	9.555	3.1
1.865	2.3	4.44	2.6	7.015	2.9	9.63	3
1.9	2.3	4.515	2.6	7.115	2.8	9.69	3.1
1.965	2.4	4.565	2.6	7.15	2.8	9.775	3.1
2.025	2.4	4.625	2.6	7.21	2.8	9.825	3
2.095	2.3	4.695	2.7	7.285	2.9	9.875	3.1
2.16	2.4	4.77	2.6	7.345	2.8	9.945	3.1
2.23	2.4	4.83	2.7	7.43	2.8	10.005	3
2.305	2.4	4.905	2.6	7.47	2.9	10.07	3.1
2.355	2.3	4.93	2.5	7.54	2.8	10.155	3.1
2.415	2.3	5	2.5	7.625	2.9	10.19	3.1
2.465	2.3	5.075	2.7	7.65	2.9	10.25	3.1
2.535	2.4	5.15	2.6	7.75	2.8	10.325	3.1

Table A.2: Current Vs. Voltage measurement for Old Laxapana GVPI stator

V(kV)	I(µA)
10.38	3.1
10.45	3.1
10.51	3.1
10.57	3.1
10.66	3.2
10.73	3.2
10.77	3.1
10.84	3.2
10.89	3.1
10.93	3.2
11.02	3.1
11.08	3.2
11.16	3.2
11.21	3.2
11.3	3.2
11.34	3.1
11.4	3.2
11.46	3.2
11.52	3.2
11.58	3.3
11.63	3.2
11.73	3.3
11.74	3.2
11.82	3.3
11.89	3.2
11.95	3.2
12.04	3.3
12.1	3.3
12.13	3.2
12.22	3.2
12.29	3.2
12.33	3.3
12.39	3.2
12.49	3.3
12.52	3.3
12.59	3.3
12.67	3.3
12.73	3.2
12.77	3.3
12.85	3.3

V(kV)	I(µA)
12.975	3.2
13.06	3.3
13.095	3.3
13.22	3.4
13.265	3.4
13.29	3.3
13.365	3.4
13.425	3.3
13.475	3.3
13.56	3.3
13.62	3.4
13.67	3.4
13.745	3.4
13.805	3.4
13.865	3.3
13.94	3.3
13.96	3.3
14.07	3.4
14.095	3.3
14.18	3.4
14.23	3.4
14.305	3.4
14.355	3.4
14.45	3.5
14.475	3.4
14.55	3.5
14.585	3.4
14.685	3.4
14.73	3.5

Table A.3: Current Vs. voltage measurement data for Wimalasurendra stator

V(kV)	I(μA)	V(kV)	I(μA)	V(kV)	I(μA)	V(kV)	I(μA)
0.045	1.1	2.49	6.6	4.965	7.9	7.42	8.9
0.095	4	2.56	6.6	5.025	7.9	7.47	8.9
0.145	4.2	2.635	6.7	5.075	7.9	7.54	9
0.23	4.4	2.685	6.6	5.125	8	7.6	9
0.265	4.5	2.73	6.7	5.21	8	7.69	9.1
0.325	4.7	2.795	6.7	5.27	8	7.725	9.1
0.4	4.7	2.88	6.8	5.345	8.1	7.8	9.1
0.475	4.8	2.94	6.8	5.405	8	7.87	9.1
0.52	4.9	3.015	6.8	5.455	8.1	7.92	9.1
0.595	5	3.085	6.9	5.525	8.1	7.98	9.1
0.655	5	3.135	6.9	5.575	8.2	8.055	9.2
0.72	5.1	3.185	7	5.65	8.2	8.115	9.2
0.765	5.2	3.245	7	5.725	8.3	8.19	9.2
0.84	5.3	3.32	7	5.785	8.3	8.25	9.3
0.9	5.3	3.39	7.1	5.845	8.2	8.31	9.3
0.975	5.4	3.44	7.1	5.905	8.3	8.36	9.3
1.025	5.4	3.515	7.2	5.98	8.3	8.445	9.4
1.095	5.5	3.575	7.3	6.03	8.3	8.495	9.4
1.155	5.6	3.625	7.2	6.1	8.4	8.58	9.4
1.22	5.7	3.685	7.2	6.15	8.4	8.615	9.4
1.28	5.6	3.745	7.2	6.225	8.4	8.675	9.4
1.34	5.8	3.845	7.3	6.285	8.5	8.75	9.5
1.4	5.8	3.89	7.3	6.335	8.4	8.8	9.5
1.485	5.9	3.94	7.4	6.42	8.5	8.885	9.5
1.56	5.9	3.99	7.4	6.48	8.6	8.945	9.6
1.595	6	4.06	7.4	6.54	8.5	9.02	9.6
1.66	6	4.125	7.4	6.615	8.6	9.065	9.6
1.745	6	4.195	7.5	6.65	8.6	9.13	9.6
1.79	6	4.27	7.5	6.725	8.6	9.175	9.7
1.855	6.2	4.33	7.5	6.795	8.7	9.265	9.7
1.94	6.2	4.38	7.6	6.87	8.7	9.325	9.7
2	6.2	4.44	7.6	6.92	8.7	9.375	9.8
2.035	6.2	4.515	7.7	6.98	8.8	9.42	9.8
2.12	6.3	4.585	7.6	7.055	8.8	9.52	9.8
2.185	6.3	4.635	7.7	7.09	8.7	9.59	9.8
2.245	6.4	4.71	7.8	7.175	8.8	9.63	9.8
2.29	6.4	4.77	7.8	7.235	8.9	9.7	9.9
2.365	6.5	4.83	7.8	7.31	8.9	9.75	9.9
2.425	6.5	4.895	7.9	7.345	9	9.825	9.9

Table A.3: Current Vs. voltage measurement data for Wimalasurendra stator

V(kV)	I(μA)
9.885	10
9.96	10
10.005	10
10.08	10
10.14	10
10.205	10
10.265	10.1
10.335	10.1
10.385	10.2
10.46	10.2
10.51	10.2
10.555	10.2
10.64	10.3
10.69	10.3
10.75	10.4
10.825	10.4
10.885	10.4
10.945	10.4
11.02	10.5
11.08	10.5
11.13	10.5
11.205	10.6
11.275	10.6
11.34	10.6
11.41	10.6
11.46	10.7
11.535	10.7
11.58	10.7
11.655	10.8
11.705	10.7
11.755	10.8
11.84	10.8
11.9	10.8
11.95	10.8
12.02	10.9
12.095	10.9
12.145	10.9
12.205	11
12.28	11
12.34	11
12.4	11
12.475	11.1
12.545	11.1
12.57	11.1
12.67	11.2
12.73	11.2
12.79	11.3
12.85	11.3
12.915	11.3
12.975	11.4
13.02	11.3
13.095	11.4
13.155	11.4
13.22	11.4
13.29	11.4
13.35	11.5
13.415	11.5
13.485	11.6
13.525	11.6
13.585	11.6
13.645	11.6
13.705	11.6
13.805	11.7
13.84	11.7
13.915	11.8
13.985	11.8
14.025	11.8
14.095	11.8
14.145	11.9
14.23	11.9
14.305	11.9
14.34	12
14.4	12
14.475	12
14.55	12.1
14.62	12.2
14.67	12.3

Table A.4 :Real part of permittivity measurements along frequency sweep

	Real part of permittivity		
Frequency	OLPS VPI stator (F/m)	OLPS GVPI stator (F/m)	WPS VPI stator (F/m)
0.0010			1.240016
0.0010		1.166985	1.239435
0.0022		1.134582	1.200160
0.0046		1.109073	1.166861
0.0100		1.087937	1.137618
0.0215		1.073242	1.113138
0.0464	1.176998	1.061175	1.093893
0.1000	1.142832	1.051189	1.078045
0.2154	1.114181	1.042573	1.064208
0.4642	1.090800	1.035455	1.051818
1.0000	1.071500	1.028869	1.040908
2.1546	1.056239	1.023147	1.031454
4.6417	1.044404	1.018009	1.023300
10.0000	1.035227	1.013514	1.016354
20.0000	1.028591	1.009868	1.011182
40.0000	1.022793	1.006771	1.006912
70.0000	1.018685	1.004570	1.004078
110.0000	1.015310	1.003001	1.002160
222.2200	1.009698	1.000991	1.000000
446.6800	1.001354	0.999930	
500.0000	1.000000	1.000000	

Table A.5 :Imaginary part of permittivity measurements along frequency sweep

	Imaginary part of permittivity		
Frequency	OLPS VPI stator (F/m)	OLPS GVPI stator (F/m)	WPS VPI stator (F/m)
0.0010			0.186740
0.0010		0.091105	0.185528
0.0022		0.067967	0.120325
0.0046		0.051681	0.086502
0.0100		0.039334	0.066761
0.0215		0.031462	0.054016
0.0464	0.095483	0.025486	0.045612
0.1000	0.074075	0.021116	0.035660
0.2154	0.058517	0.017635	0.029808
0.4642	0.046975	0.015065	0.025410
1.0000	0.037580	0.013010	0.021797
2.1546	0.029872	0.011503	0.018714
4.6417	0.023738	0.010107	0.015888
10.0000	0.019342	0.008838	0.013317
20.0000	0.016893	0.007811	0.011252
40.0000	0.016139	0.006957	0.009486
70.0000	0.016944	0.006397	0.008322
110.0000	0.018889	0.006053	0.007604
222.2200	0.024947	0.006064	0.007282
446.6800	0.035943	0.006923	
500.0000	0.038453	0.007149	

Table A.6 :Dissipation factor measurements along frequency sweep

	Dissipation Factor		
Frequency	OLPS VPI stator	OLPS GVPI stator	WPS VPI stator
0.0010			0.1505946
0.0010		0.078068	0.1496875
0.0022		0.059905	0.1002574
0.0046		0.046599	0.0741323
0.0100		0.036154	0.0586851
0.0215		0.029315	0.0485258
0.0464	0.081125	0.024016	0.0416974
0.1000	0.064817	0.020087	0.0330787
0.2154	0.052520	0.016915	0.0280093
0.4642	0.043065	0.014549	0.0241581
1.0000	0.035073	0.012644	0.0209408
2.1546	0.028281	0.011242	0.0181429
4.6417	0.022729	0.009928	0.0155266
10.0000	0.018684	0.008720	0.0131026
20.0000	0.016423	0.007735	0.0111279
40.0000	0.015780	0.006910	0.0094208
70.0000	0.016633	0.006368	0.0082881
110.0000	0.018604	0.006035	0.0075874
222.2200	0.024707	0.006058	0.0072816
446.6800	0.035895	0.006923	
500.0000	0.038453	0.007149	

Appendix-B

1. Parameter estimation for OLPS GVPI Stator using MATLAB

General model: F (x) = 16.67*(x/b+0.110+ (d*0.110*x^(1-n))/(1-n))

Coefficients (with 95% confidence bounds):

b = 9864 (7633, 1.209e+04)

d = 0.006457 (0.003917, 0.008997)

n = 0.7312 (0.292, 1.17)

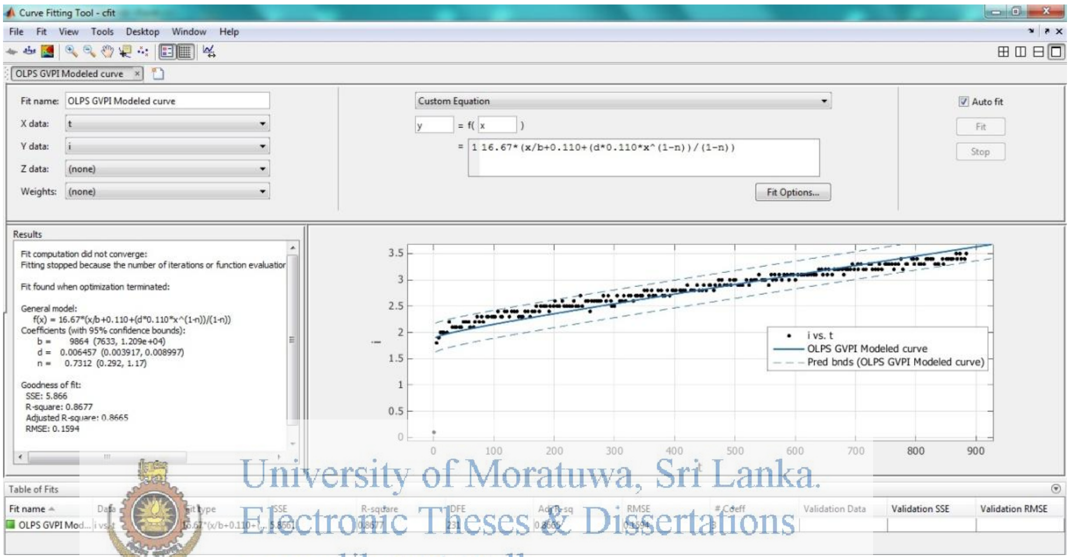

Figure B.1: MATLAB workspace - Curve Fitting tool

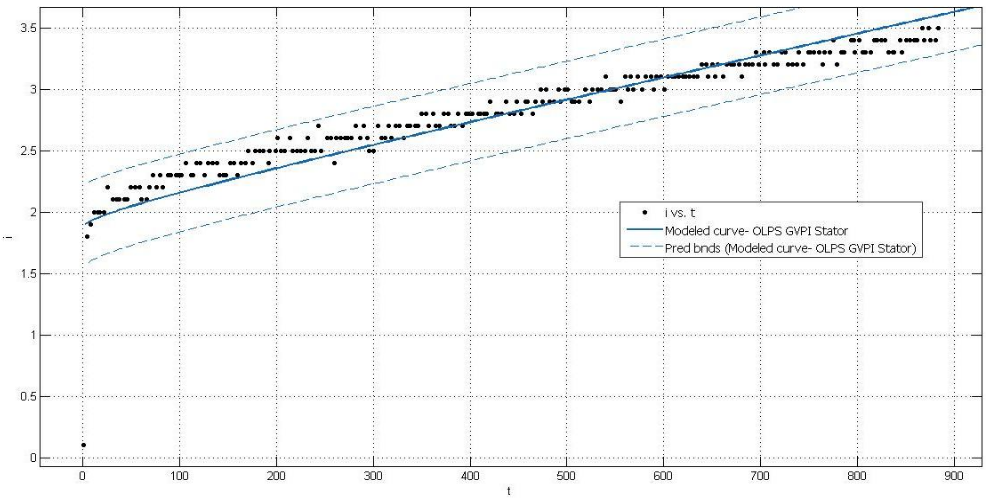

Figure B.2: Modeled curve within 95% prediction boundaries

2. Parameter estimation for OLPS VPI stator using MATLAB

General model: F (x) = 16.67*(x/b+0.0914+(d*0.0914*x^(1-n))/(1-n))

Coefficients (with 95% confidence bounds):

b = 4352 (4221, 4484)

d = 0.07112 (0.07024, 0.07201)

n = 0.7408 (0.7256, 0.7559)

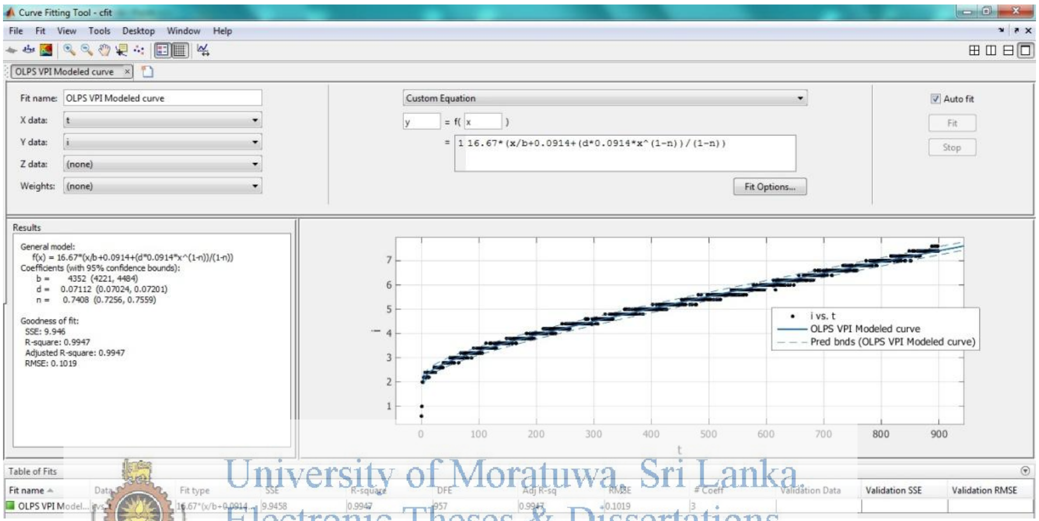

Figure B.3: MATLAB workspace- Curve fitting tool

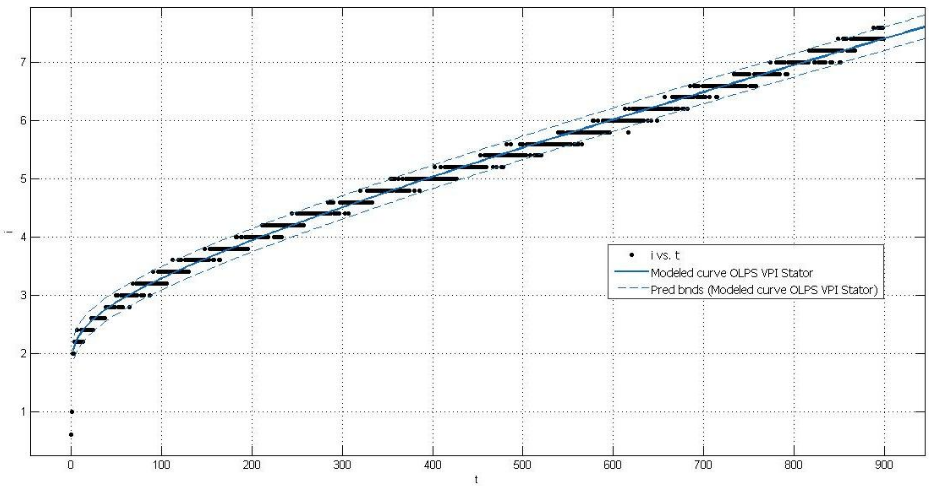

Figure B.4: Modeled curve within 95% prediction bounds

3. Parameter estimation for WPS VPI Stator using MATLAB

General model:

f(x) = 16.67*(x/b+0.158+(d*.158*x^(1-n))/(1-n))

Coefficients (with 95% confidence bounds):

b = 2580 (2524, 2636)

d = 0.07529 (0.07456, 0.07602)

n = 0.7954 (0.7844, 0.8063)

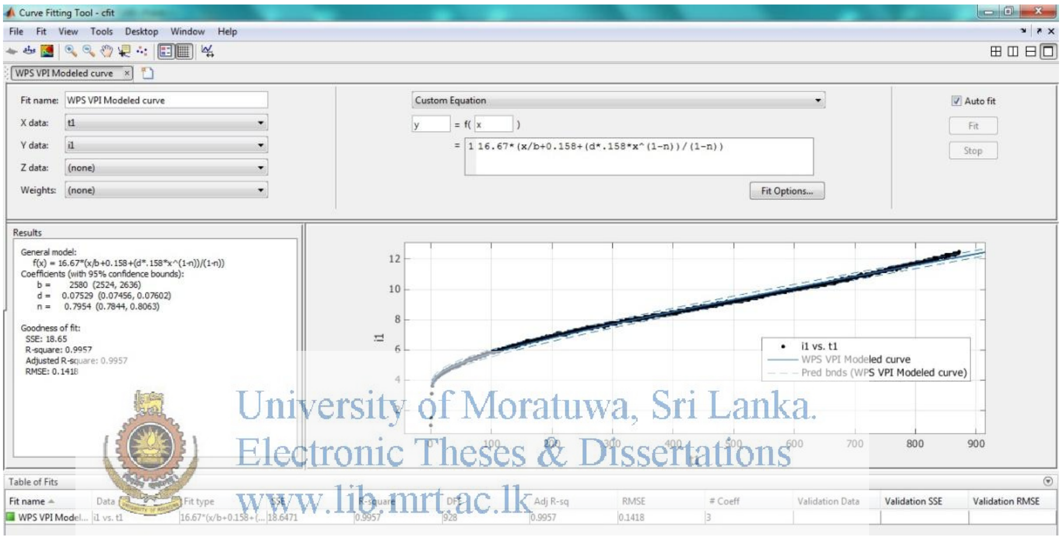

Figure B.5: MATLAB workspace - Curve fitting tool

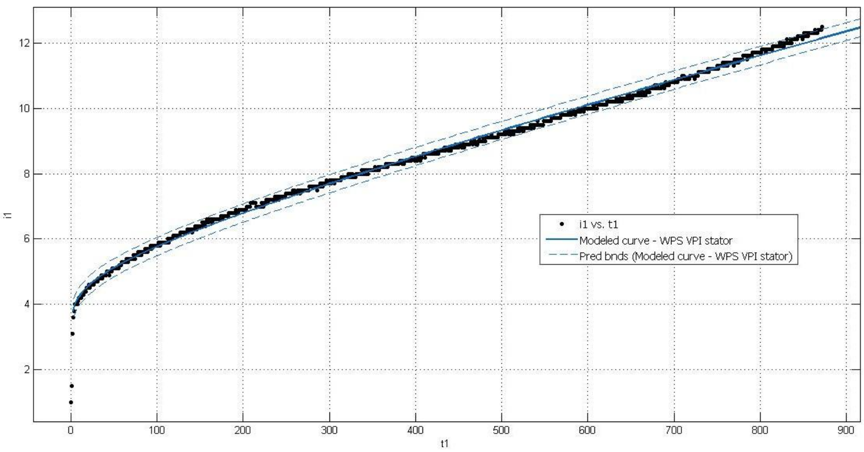

Figure B.6: Modeled curve within 95% prediction boundaries

Appendix-C